Chapter 3: Experimentation

Part – I

3.1 Gas metal arc welding of ferritic stainless steel

3.1.1 Introduction

The objective of this work was to perform GMAW of ferritic stainless steel and then, to improve the property of weld obtained after GMAW, FSP was to be carried out. This study thus consists of extensive experiments along with their detailed analysis of results. In this section, the experimentation procedure of the GMAW and sample preparation for characterizing the welded plates have been discussed. An experimental setup was also developed to perform the experiment that included a torch holding device, copper backing plate and clamping device to fix the job for the welding operation. The setup was designed to ensure that the repeatability is good so that the chances of error can be reduced to a minimum level. The development of setup, particularly for GMAW, was essential to minimise human error during welding experiments. The welded plates at different welding process parameters were characterized using various characterisation techniques, including microstructural examination, hardness, tensile testing and Charpy impact testing. The welded samples were also subjected to non-destructive testing such as MBN (MBN) and hysteresis loop (HL) technique. The welded plate that possessed the best combination of mechanical properties was selected for further FSP to improve the mechanical properties of the welded joint.

3.1.2 Selection of base material and welding process

The low chromium grade of AISI 409 stainless steel, i.e. AISI409L, was selected as base material due to its extensive applications in automotive and other industries. GMAW is an important fabrication technique in these industries and is a well-established process for welding stainless steels. The process of GMAW is well suited for welding of even thick sections of stainless steel. However, this material in welded condition possessed some problems which were planned to be overcome by the FSP technique in this work. The material was procured from a reliable vendor in a thickness of 3.0 mm. From the plates procured, samples of size 100×50×3 mm were produced by sheet metal cutting operation. The vendor provided the mill report of the plates; however, the chemical composition was rechecked in the lab using a spark spectroscopy machine. Table 3.1 shows the chemical composition of the base material as obtained from spark spectroscopy.

Table 3.1 Chemical compositions of base metal (weight %)

Material	C	Mn	Si	S	P	Cr	Ni	Cu	Mo	Nb	Ti	N
SS409L	0.024	0.263	0.517	0.001	0.023	11.24	0.066	0.01	0.006	0.04	0.234	0.027

3.1.3 Selection of electrodes

The type of electrode selected for manufacturing plays a very important role in deciding the mechanical properties of the weldment. As stated earlier in the literature review section that generally, austenitic grades of electrode are used for welding of ferritic stainless steel grade material. On performing the welding operation of ferritic stainless steel with the austenitic grade of electrode, the formation of different phases like austenite, martensite, ferrite and some precipitates (carbides and nitrides of Cr, Ti, Mo, etc.) occur. These different phases tend to restrict the growth of the ferrite phases of the WMZ; therefore, finer grains can be achieved in the WMZ. As it is well known that finer grains possess better mechanical properties than coarser grains.

Therefore, in this study, an austenitic grade of electrode material (ER304L) have been used. The diameter of the electrode wire was 1.2 mm. The spool of the electrode was purchased by a reliable vendor (Caston electrode company, Delhi). The weight of the spool was 12.5 kg.

The chemical composition of the electrode is shown in Table 3.2.

Table 3.2 Chemical compositions of electrode wire (weight %)

Material	C	Mn	Si	S	P	Cr	Ni	Cu	Mo	Nb	Ti	N
ER304L	0.015	1.65	0.243	0.013	0.031	18.46	8.14	0.434	0.352	0.05	0.008	0.22

3.1.4 Selection of backing plate

To support the molten weld metal from flowing out during welding, a plate below the base metal is used, which is known as the backing plate. Depending upon the type of welding process, this plate may be fused with the workpiece (fusible backing plate) or may not be used (non-fusible backing plate). Generally, the material of the fusible backing plate is same as that of the workpiece material, whereas it is not the case with the non-fusible backing plate type. The advantage of the non-fusible backing plate is that it can be used again and again. Other methods are also applied to prevent the molten weld pool from flowing down, such as root backing, backing with submerged arc welding flux and weld backing. The type of method used for backing depends on the type of welding process being used.

In the GMAW process, generally, the non-fusible backing plates are used. Apart from supporting the molten weld pool, the non-fusible backing plate also helps to conduct some of the heat of the weld to itself. Thus, the amount of heat transferred to the un-melted portion of the base material is reduced. This, in turns, restricts the width of the HAZ, and also the amount of grain coarsening that happens in the coarse grained region of the HAZ is also reduced. Pure copper is generally used as a non-fusible backing plate for the GMAW process. The high thermal conductivity of copper and copper-based alloys is not only helpful in preventing the copper plate from melting and is very effective in transferring the heat away from the welded region. Some other materials apart from copper and copper alloys like aluminium and aluminium alloys have also been tried as an alternative for pure copper, but the poor weld quality has been reported due to the lower melting point and lesser thermal conductivities of these materials.

To ensure through melting of the weld metal up to the bottom of the workpiece material, a groove is provided on the top surface of the backing plate to allow the molten metal to flow up to the root of the joint. The dimensions of the groove, i.e. the width and thickness, depends upon the thermal conductivity and dimensions of the work piece material being welded. The thicker the base material, the wider will be the groove. For properly working of the backing plate, the scale or dust must be removed before welding operation.

In this experiment, the backing plate of copper has been used having dimensions (200 × 120 × 10 mm) which is shown in Figure 3.1.

Figure 3.1 Copper backing plate.

3.1.5 Joint configuration

Different applications require different types of welding joints. There are mainly five types of welding joints (lap, corner, edge, tee and butt joint) which are shown in

Figure 3.2 [162]. Each type have different variations also. The selection of the welding joint depends upon many factors such as the thickness of the plate; forces applied on the joint, applications of the joint and several other factors.

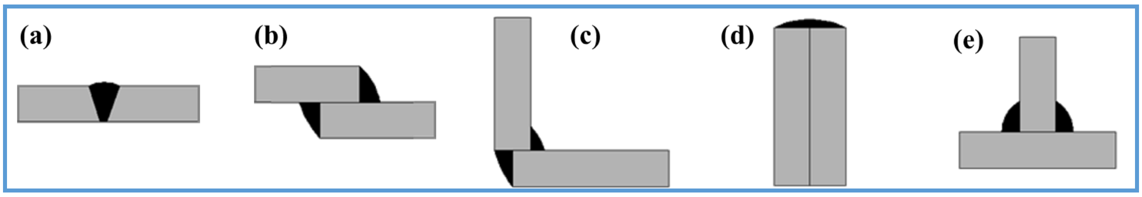

Figure 3.2 Different types of joints: (a) butt joint, (b) lap joint, (c) corner joint, (d) edge joint, and (e) tee joint.

Lap joint: In this type of joint, the two plates are placed on each other in an overlapping manner. This joint is generally used for the joining of materials having different thicknesses. This joint is commonly used for sheet metal. The welding of thicker sections is not preferred in this configuration.

Corner joint: In this joint configuration, the two plates are placed perpendicular to each other, and their edges come together. This configuration is primarily used in the manufacturing of boxes and frames.

Edge joint: In this type of joint, the two plates are placed together such that their edges come side by side.

Tee joint: In this joint, the two plates are placed perpendicular to each other, and the location of one plate should be in the centre of the other plate.

Butt joint: In this type of configuration, both base plates to be welded are placed together in the same plane and joined by their sides. It is the widely used joint configuration in the fabrication of structures and piping systems because this joint can be easily prepared, and also it has different variations, which are shown below in Figure 3.3 [163].

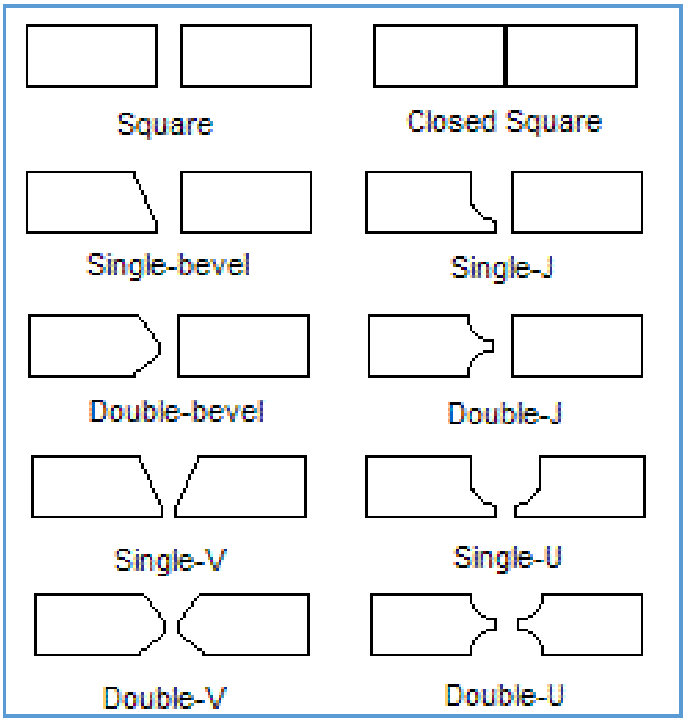

Figure 3.3 Types of the butt joint.

The selection of any one type of butt joint among these different variations depends upon various factors, in which, the thickness of the base material to be welded is one of the essential factors. Closed square and square type of butt joint are used for thinner materials (thickness less than 6.0 mm). All other variations are used for thicker sections.

For this study, the square butt welding has been selected as the joint configuration because the thickness of the material is only 3.0 mm.

3.1.6 Equipment used for experimentation

In this study, mainly two different machines were used. One is the GMAW machine setup, and another is the FSP machine setup. The machine specifications and the salient features of both the machines have been described below. The components associated with each machine is also described one by one in the following sections.

3.1.6.1 Gas metal arc welding machine

GMAW machine setup that was used in this work is shown in Figure 3.4. The welding machine used was of ADOR-MAXI MIG 251. This machine setup consists of different components such as welding gun and wire feed unit, power supply, electrode, electrode holder, shielding gas, welding trolley, rail and clamping set up to perform successful welding operation. This machine setup takes a lot of space; therefore, all components of this machine cannot be captured in one image; hence two images Figure 3.4(a) and Figure 3.4(b) are required to show its components. The details of each of these components have been described below in their respective sections.

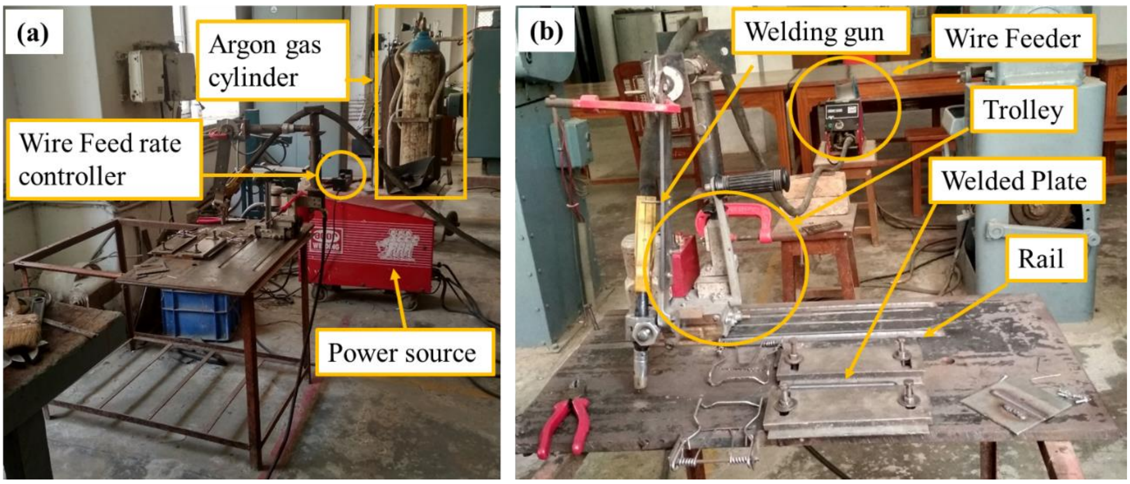

Figure 3.4 GMAW machine setup along with its components: (a) shielding gas cylinder, wire feed rate controller, power source, and (b) welding gun, wire feeder, welding trolley, welding rail, welded plate.

3.1.6.2 Power supply

In this study, a constant voltage power source is used since GMAW welding carried out is a semiautomatic type. In the GMAW setup, the electrode is continuously fed according to the welding process parameters such as welding voltage and wire feed rate. The feeding of the electrode is not controlled by the operator independently during the welding operation. Due to the consumable nature of the electrode, the distance between the electrode tip and workpiece may vary continuously, and to maintain the arc stability, the distance between the electrode tip and workpiece should be kept constant. To maintain a consistent gap, when the distance between the electrode and work piece decreases, a higher amount of current is drawn from the constant voltage (CV) power source and melts the electrode at a higher rate such that the gap again increases to its previous value. On the other hand, if the gap increases, the lower amount of current is drawn to reduce the rate of melting of the electrode. The CV power source can change the welding current by a significant amount for even a small change in welding voltage (or electrode to workpiece distance). Therefore, constant voltage power supply is used in the GMAW setup.

The essential technical specifications of the welding power source are shown in Table 3.3.

Table 3.3 Specifications of the power source.

Process parameter	Range
OCV (max)	16-36 V
Range	Up to 250 A
Supply	415 V
Input	14 A
MCWC	60% DC 250 A
MCAWC	100% DC 195 A

Direct current was used with the electrode as positive polarity and workpiece as negative polarity. Direct current is preferred over the alternating current when arc stability is more important because in alternating current, polarity changes continuously with the voltage dropping to zero in each cycle of alternating current. The electrode is selected as positive polarity because, in the GMAW process, the electrode is consumable and melts in the arc. When the electrode is connected to the positive terminal, the electrons emitted from the negative terminal (workpiece) hit the electrode and lose their kinetic energy. Hence more heat is produced at the electrode, which increases the electrode deposition rate and the welding productivity.

The power supply system used in this study was a welding transformer rectifier type. The low current AC from the main supply is converted into the high current DC with the help of various components such as a step-down transformer, rectifier and filter housed within the power supply system. The alternating current of higher voltage is reduced into the lower voltage close to the operating condition with the help of a step-down transformer. The rectifier converts this low voltage alternating current into the direct current with the use of diodes. To obtain the constant voltage and current power supply, the string of pulses must be removed, and it can be done by the filter.

There are some knobs on the panel of the power supply system to set the welding process parameters. The knobs for setting the OCV can be adjusted for coarse and fine setting to set the open circuit voltage. The other knobs present are used for the gas check, pause time and spot time. Also, display of voltage (open circuit voltage, as well as welding voltage and welding current (short circuit current as well as welding current)), is on the panel. The 2 track and 4 track selector is used for generating the welding arc continuously by pressing the trigger button located in the welding gun continuously or not, respectively. When the 2 track knob is used, it is required to continuously press the trigger button on the welding gun to operate the welding operation. But when the 4 track knob is used, it is not required to continuously press the trigger button, instead of that, trigger is pressed to start the arc, and the trigger is released. When the welding is to be ended, the trigger switch on the welding torch is again pressed to extinguish the arc. To check whether the gas is properly flowing through the nozzle to the weld area or not, OCV and gas check knob are used. By using the combination of the coarse and fine knob, the open circuit voltage is accurately set. The GMAW setup can also be used for spot welding and to perform spot welding; two knobs, i.e. pause time and spot time, are used. The spot time knob is used to set the time of current drawn for a single spot weld. The pause time knob is used to fix the time during which current is not flowing in the circuit between two different spot welds.

3.1.6.3 Shielding gas cylinder

In this study, argon is used as the shielding gas. The shielding gas is stored in the gas cylinder. A flow meter and a pressure gauge are attached to this cylinder. The rate of flow of shielding gas is controlled by the flow meter on which the scaling of the flow rate is mentioned in L/min, and the rate of shielding gas is indicated by the ball floating inside the flowmeter. Pressure gage indicates the pressure of the shielding gas inside the cylinder. A key is used to open and close the flow of shielding gas from the cylinder.

3.1.6.4 Welding gun and wire feed unit

The welding gun is an integral part of the GMAW machine. It is used to continuously feed the consumable electrode in the welding arc, and the molten electrode material is deposited at the welding joint. It also allows for the flow of shielding gas in the proper amount right at the region of welding. To perform this function, a welding gun is manufactured correctly and consists of various parts like a control switch, a contact tip, a power cable, a gas nozzle, an electrode conduit and liner, and a gas hose. The generation of electric arc and extinguishing the welding arc can be controlled by pressing the control switch present on the welding gun in the 'on' and 'off' position depending upon the requirement. The pressing 'on' of the control switch, starts the feeding of the electrode wire, electric power begins to flow in the electrode along, and the flow of shielding gas starts simultaneously. It is very useful for proper maintenance of the arc and the shielding of the weld right from the very beginning of the welding. The transfer of current from the welding cable to the electrode is facilitated by the contact tip, made up of copper based material. The shape of the contact tip is nearly cylindrical, with a passage/hole in the middle throughout its length to allow the electrode to pass through it. The diameter of the inner hole is kept the same as that of the electrode to be used. It ensures that the electrode can pass through, maintaining proper electrical contact with the contact tip. To control the flow of the shielding gas into the region of the weld pool, a gas nozzle is used, which is generally made up of copper based alloys. The electrode wire is fed from the wire feeding unit to the contact tip through the liner to protect the electrode from bending. The gas is passed through the gas hose from the gas cylinder to the contact tip. After that, the gas flows around the contact tip and is channelized/constricted in the nozzle. It ensures that the proper flow of gas is maintained around the arc during welding.

The wire feeding unit consists of a roller to drive the electrode into the liner, a feeder button, and a wire feeder panel. The electrode is in the form of a spool, which can continuously rotate during the welding process as and when required. A motor drives the drive rollers. The speed of the rollers is varied so that the rate of wire feed is the same as the rate at which it is melted in the welding arc. A feeder button can be used to manually feed the electrode during the setting up of the new spool of the electrode before the welding operation. The wire feeder panel controls the feed rate.

3.1.6.5 Welding trolley

To perform the welding operation, the welding gun can be held manually or by some mechanical means. In the manual holding of the welding gun, there are chances of human error in properly maintaining the gap between the electrode tip and workpiece, torch angle, and welding speed, which may reduce the arc stability and result in the bad quality of the welds. To improve the weld quality by minimizing the human involvement, the welding gun was mounted on the extended part of the welding trolley by mechanical joints, as shown in Figure 3.5.

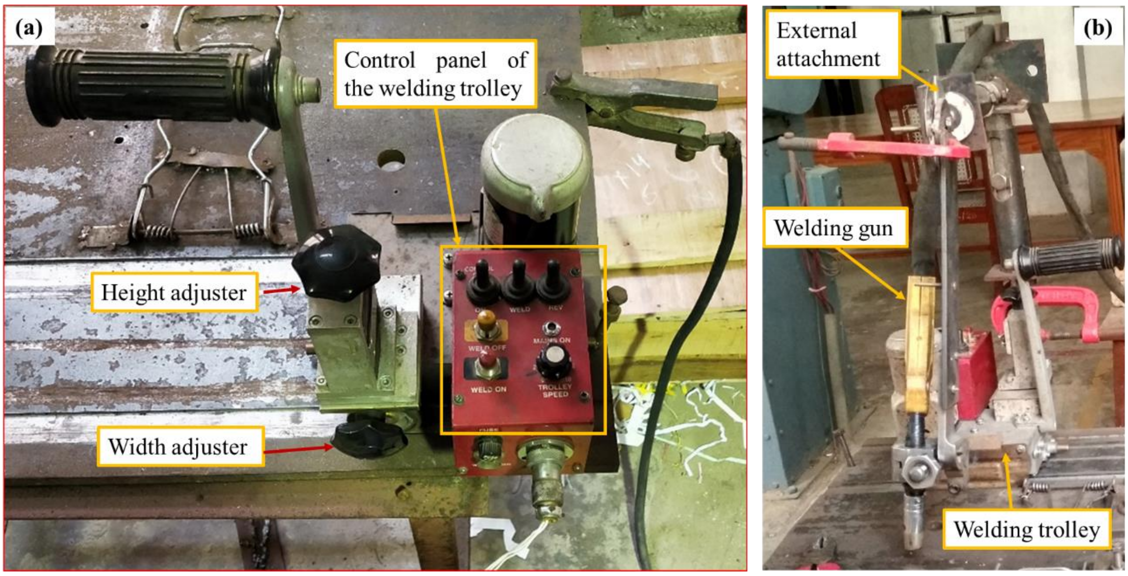

Figure 3.5 Welding trolley: (a) controller components, (b) attachments to the welding trolley.

In such type of arrangement, the welding gun can also be fixed at the required angle to the base plate. The power supply is given to the motor which drives the trolley. An arrangement (height adjuster) is provided on the trolley to vary the height of the welding gun above the workpiece. Also, the position of the welding gun can be adjusted across the width of the base metal by the width adjuster. The panel of the welding trolley consists of some press buttons to perform the welding operation. These buttons are ‘trolley off’ and ‘trolley on’, ‘mains on’, ‘set’ and ‘weld’, ‘forward’ and ‘reverse’ switch for deciding the direction of motion, ‘weld off’, ‘weld on’, and a knob to set the trolley speed. The ‘control off’ and ‘control on’ button controls the flow of current to the trolley. When the button is on the ‘control on’ mode, the flow of current is also indicated by the red light on the ‘mains on’ button. To start and stop of the welding trolley movement, ‘weld-on’ button and ‘weld-off’ button is pressed, respectively. When the trolley is required to be moved to set the path of welding, ‘set’ mode is switched on and when the welding trolley is to be moved during the welding operation, ‘weld’ mode is switched on. The trolley is capable of moving in the forward direction as well as in the backward direction. To move the trolley in the forward direction, the toggle switch is turned towards the ‘forward’ direction and to reverse the trolley, the switch is positioned in the other direction. The speed of the trolley is controlled by turning the ‘trolley speed’ knob.

3.1.6.6 Welding rail

The welding trolley moves in the predetermined straight path to perform the welding in a straight line. This straight path is known as welding rail, which is shown in Figure 3.6.

Figure 3.6 Welding rail.

In this study, the welding rails were manufactured by cutting grooves within the upper plate of the mild steel workbench. The width of the groove on the work bench was kept to properly fit the wheels of the welding trolley. It further ensured that the trolley moves in the predetermined straight path with no deviations. The length of the rail was kept sufficient to weld plates of various lengths. While travelling, the trolley may fall off after covering the length of the rails. To prevent it from falling off, a stopper was placed at one end of the work bench so that it pressed the stop button provided in the welding trolley and thus stopped the welding trolley at the end of the work bench.

3.1.6.7 Job clamping setup

The clamping of the work pieces during the welding operation is one of the most crucial steps. In the welding process, a high amount of thermal stresses are produced, which tend to distort the welded component. To prevent unwanted distortion in the welded component, the clamping must be appropriately rigid. The clamping setup used in this study is shown in Figure 3.7.

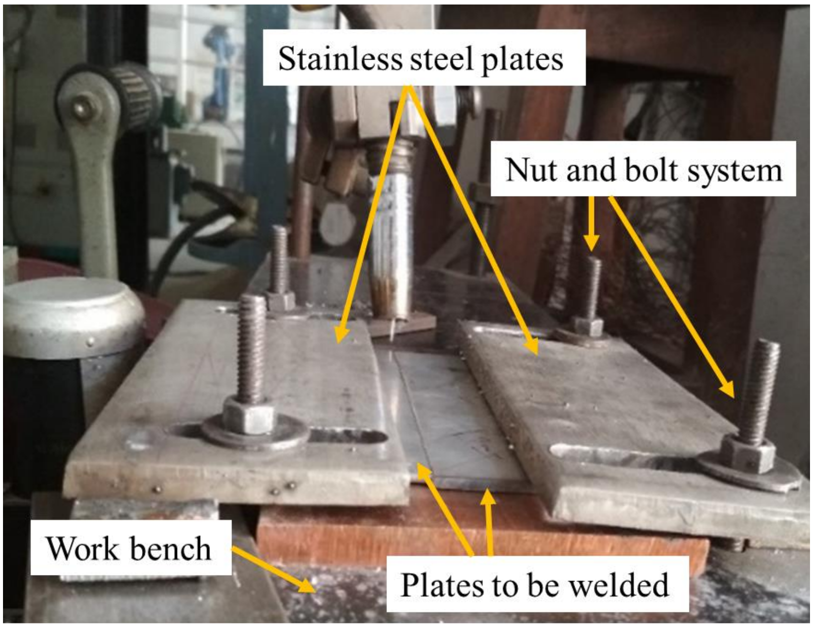

Figure 3.7 Job clamping setup.

From this figure, it can be seen that the job clamping setup was placed on the work bench itself, and stainless steel plates have been used to clamp the workpiece with the help of nut and bolt. The work pieces are put on the copper backing plate, and then clamping of the workpieces are performed by the stainless steel plates.

The complete specifications of the GMAW machine (**ADOR MAXI MIG-251**) used for the whole experimentation is given in Table 3.4.

Table 3.4 Specification of the GMAW machine.

Technical parameters	**Description**
Rated travel speed of the welding trolley	1500 mm/min
Rated wire feed rate	18 m/min
Rated current value	400 ampere
Rated voltage	60 volt

3.1.7 Welding trial runs for gas metal arc welding of SS 409L

Before final experimentation, a parametric window of welding process parameters should be known wherein the welding is possible. To find this range of welding process parameters, extensive trial runs are performed on the base material. First, the trial runs were carried out using the ‘bead on plate’ technique of welding and different welding process parameters like wire feed rate, open circuit voltage, and welding speed were varied one at a time. Second, the trial runs were also performed to weld two plates of SS409L. The root gap and shielding gas flow rate were established using this second set of experiments. After performing several trial runs, the range of welding process parameters was established, and final experimentation was carried out in this process parameter range. Few defects were observed during the bead on plate trial run, such as spattering, more height of reinforcement, no arc generation, wider weld bead, and very narrow weld bead. However, it was observed that during the ‘bead on plate’ trial runs, fewer defects were observed as compared to the case when welding of two plates. Therefore, the process parameters were selected so that no defects occurred during the final experimentation.

3.1.7.1 Criterion for determination of process parametric window

Apart from the apparent criterion like lack of fusion and undercut, the following criterion was used for the determination of process parametric window

3.1.7.1.1 Spattering

During the welding process, melting of both the parent metal and electrode wire occur. Due to the involvement of high temperature together with the arc forces, magnetic forces and gas pressures, reactions often become volatile, which deflects some amount of molten metal out of the welded area in the form of tiny drops. On coming in contact with the cold base material on either side of the weld, these drops solidify and get stuck on the surface of the base material. Such type of solidified drop is known as spatter. Spatter cannot be totally eliminated in the GMAW process; however, it can be minimized by reducing the cause of spattering.

Cause of spatter:

(i) Welding current: Too high wire feed rate or welding current may cause spattering phenomenon.

(ii) Welding voltage: Low value of welding voltage will create spatter.

(iii) Electric stick out (ESO): It is the distance between the contact tip of the electrode and the upper surface of the base material. Too high ESO will generate spatter.

(iv) Surface contaminants: Various surface contaminants like rust, oil, paint, etc., can cause spatter. That is why, the material should be cleaned to eliminate or minimize the spattering.

(v) Fluctuation in wire feeding: Due to intermittent feeding of the electrode by the wire feeder, it result in the variation of welding current and causes a lot of spatter.

(vi) Bad Shielding Gas: The purity and the type of the shielding gas may affect the amount of spattering. High purity argon causes less spattering, while pure carbon dioxide causes more amount of spatter. However, argon is costlier than carbon dioxide. Impurity in shielding gases make the arc more volatile and result into the increase in spatters.

3.1.7.1.2 Inappropriate weld bead shape

Welding process parameters are the controlling factor that affects the weld bead geometry (bead width, bead height and penetration). Weld bead geometry are a very important factor to determine the quality of the joints. The width of the weld bead should be small but must be wide enough to melt a sufficient portion of the base material. The weld joints should have a width of the weld bead to penetration ratio between 1.2 to 2.0 to possess good weld strength. The width of the weld bead depends upon welding process parameters such as welding speed, welding current, welding voltage, gas flow rate, electrode diameter, nozzle to tip distance, etc. It is generally seen that the width of the weld bead increases with the increase in welding current, welding voltage, gas flow rate, electrode diameter, contact tip to work distance. The reason for the variation in the width of the weld bead is the variation in the distribution of heat between the base metal and electrode wire. On increasing welding speed, keeping all other parameters constant, the base metal received less heat input per unit length. Due to this reduced heat input, less melting of the base metal takes place, and deposition of the filler metal per unit length was also reduced due to faster movement of the welding torch. Due to less melting of the base metal as well as less deposition of the filler metal, the smaller weld bead is formed.

Bead height is the height of upper reinforcement. To obtain good quality of the weld joints, it is necessary to avoid the production of very thick weld bead because it may cause distortion, burn-off at the edge, deep craters at the end, sagging of the weld pool as well as wastage of energy and filler wire. Due to larger bead height, the junction point of the upper reinforcement and surface of the base metal (also known as weld toe) is not smooth, and produces a notch effect. The notch effect (size effect) deteriorates the properties of the welded joints. Therefore it is necessary to produce welds having smaller bead height by proper selection of the welding process parameters. Bead height decreases with the welding speed. It was due to the fact that on increasing welding speed, the heat input per unit length given to the base metal is reduced and also deposition of the filler metal is reduced due to high welding speed.

Penetration is the distance measured perpendicular from the upper surface of the base metal to the deepest part of the weld metal. Ideally, penetration should be equal to the thickness of the base metal; however, excess penetration up to a certain amount is also acceptable. The limit of the acceptance of excess penetration depends upon the type of metals, type of welding methods, type of joints, application of welded joints, etc. Beyond the acceptable limit, excess penetration is not desired because, apart from causing wastage of energy, it can lead to excessive flow of liquid weld metal near the weld root. It deteriorates the quality of the product and increases the weight of the product and wastage of filler metal, which results in a reduction in productivity. Penetration depends upon the heat input provided to base metal per unit length which in turn depends upon the welding process parameters. More heat input per unit length provided to the base metal causes more melting of the base metal, resulting in more penetration. Due to the faster electrode movement by increasing the welding speed, lesser heat input was received by the base metal per unit length. It causes a reduction in the melting of base metal, which resulted in reduced penetration with an increase in welding speed.

3.1.7.1.3 No arc generation

To generate the arc, proper selection of welding parameters plays an important role. The voltage difference across the arc depends upon the open circuit voltage and arc length. The larger the arc length, the larger the voltage difference, but current will be reduced drastically due to the increase in the electrical resistance to the current flow with the increase in arc length. After increasing the arc length beyond a specific limit, the current flow is reduced to such a level that generation of arc is difficult, and the arc is extinguished.

3.1.7.2 Determination of the range of welding process parameters

The range of welding process parameters such as open circuit voltage, wire feed rate, welding speed, nozzle to plate distance, root gap, shielding gas flow rate has been determined by carrying out extensive trial runs.

3.1.7.2.1 Open circuit voltage

When there is no electrical load, the voltage between the two terminals is known as the open circuit voltage (OCV). In GMAW, one terminal is electrode wire, and another is base material to be welded. The no load means absence of arc between these electrodes. Power supply possesses its own V-I characteristics at different values of OCV. On increasing the OCV, the welding voltage also increases for the given value of current. The welding power supply used in this study possessed a maximum OCV of 32 volt. Higher OCV results in higher heat generation, which may deposit more filler material, and below a lower OCV may result in no arc generation. Therefore, the range of OCV was established for proper arc generation with the help of various trial runs. It was observed that this range of OCV was 26 to 30 volt. Three values of OCV (26, 28 and 30 volt) were selected for performing the experimentation.

3.1.7.2.2 Wire feed rate

The rate at which the electrode is fed into the molten weld pool is known as the wire feed rate. Some GMAW welding machines can independently control the welding current, while in other GMAW welding machines, the welding current is regulated by the wire feed rate. The higher the value of the wire feed rate, the higher will be welding current. For the present investigation, a second type of welding machine was used. Lower wire feed rate resulted in the lower welding current, and thus lower heat generated, leading to improper weld penetration, while the higher wire feed rate resulted in the higher filler metal deposition, which may add excessive reinforcement. Therefore, the range of wire feed rate should be established appropriately.

In this study, the range of the wire feed rate was found after extensive trial runs, and the value of this parameter was found between 3 m/min to 5 m/min. For this study, three values of wire feed rate (3, 4 and 5 m/min) were selected to perform the welding operation.

3.1.7.2.3 Welding speed

The speed at which the welding torch moves with respect to the workpiece is known as welding speed. The heat input per unit volume of the base material largely depends upon the welding speed. The total heat generated at any point depends upon the welding current, welding voltage, time and welding efficiency. But the distribution of this total heat input per unit volume along the weld line depends upon the welding speed. Lower the welding speed, more accumulation of heat will occur per unit volume of material, while on increasing the welding speed, the heat is quickly distributed over a longer length which reduces the heat input per unit volume. Welding speed is thus an important process parameter that needs to be controlled in a specific range.

In this study, after carrying out several trial runs, the welding speed range has been found and lies between 240 mm/min to 500 mm/min. However, out of this range of welding speed, only two values of welding speeds (400 mm/min and 500 mm/min) were selected for performing the experimentation.

3.1.7.2.4 Nozzle to plate distance (stand-off distance)

For producing quality welds, the setting of weld parameters should be done attentively. There are some welding terms (electrode extension, stick-out, contact tip setback, stand-off distance and contact tip to workpiece distance) about which people often get confused, which may lead to poor quality of the weld. Therefore, the difference between these welding terms can be easily seen from the schematic diagram, shown in Figure 3.8 [164].

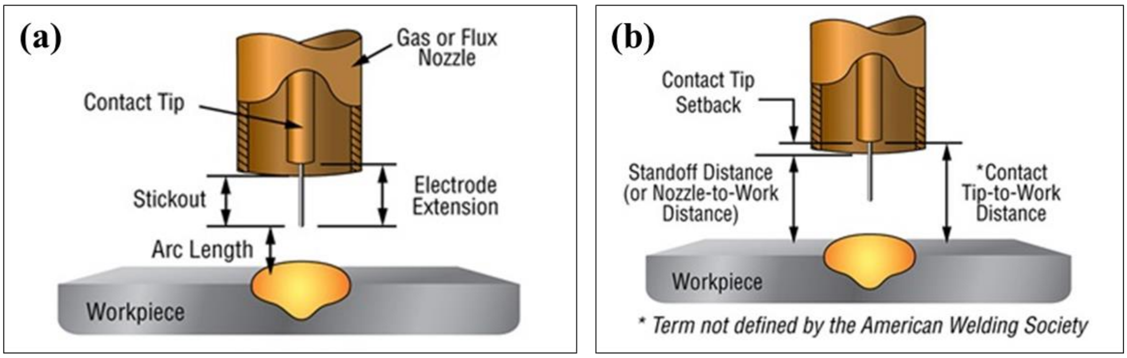

Figure 3.8 Schematic diagram of (a) stick out and electrode extension, (b) nozzle to workpiece distance and contact tip to workpiece distance.

The difference between these terms is also described below.

Stick-out: The distance between the end of the nozzle to the end of the electrode wire from where the wire melts off.

Contact tip set back: It is the distance between the end of the nozzle to the contact tip.

Arc length: It is the distance between the workpiece surface and the end of the electrode wire.

Contact tip to work distance: It is the distance between the contact tip to the workpiece surface. It is equal to the sum of the electrode extension and arc length.

Stand-off distance: It is the distance between the end of the nozzle to the workpiece surface. It is equal to the sum of the stick-out and arc length.

In all of the terms, the contact tip to work distance is the most commonly used term in welding operations. However, its measurement is difficult because the contact tip is inside the nozzle. Therefore, another word, stand-off distance (nozzle to work distance), is commonly used due to its easy measurement. The appropriate stand-off distance must be determined in welding since it affects the quality of weld joints by the occurrence of some defects like pits and blowholes.

In this study, several trial runs were carried out to find the appropriate value of stand-off distance. Finally, 8 mm was selected as the stand-off distance for performing the welding operation at all combinations of welding process parameters.

3.1.7.2.5 Root gap

After finding the range of welding process parameters using the bead on plate technique, the trial run was also performed to weld two plates. To decide the root gap between the plates for the welding operation is one of the major tasks. Several trial runs have been performed to decide the optimum root gap. Root gap is the distance between the faces of the two plates when placed in the butt position. Root gap plays a very important role to perform the welding operation satisfactorily. A root gap is provided to ensure the weld joint with full penetration. The amount of root gap depends upon the thickness of the material and the shape of the welded joint. Root gap also facilitates the escape of gases generated during the welding process to avoid blowholes in welding.

In this study, different trial runs have been carried out to find the optimum root gap. Some of them are shown in Figure 3.9.

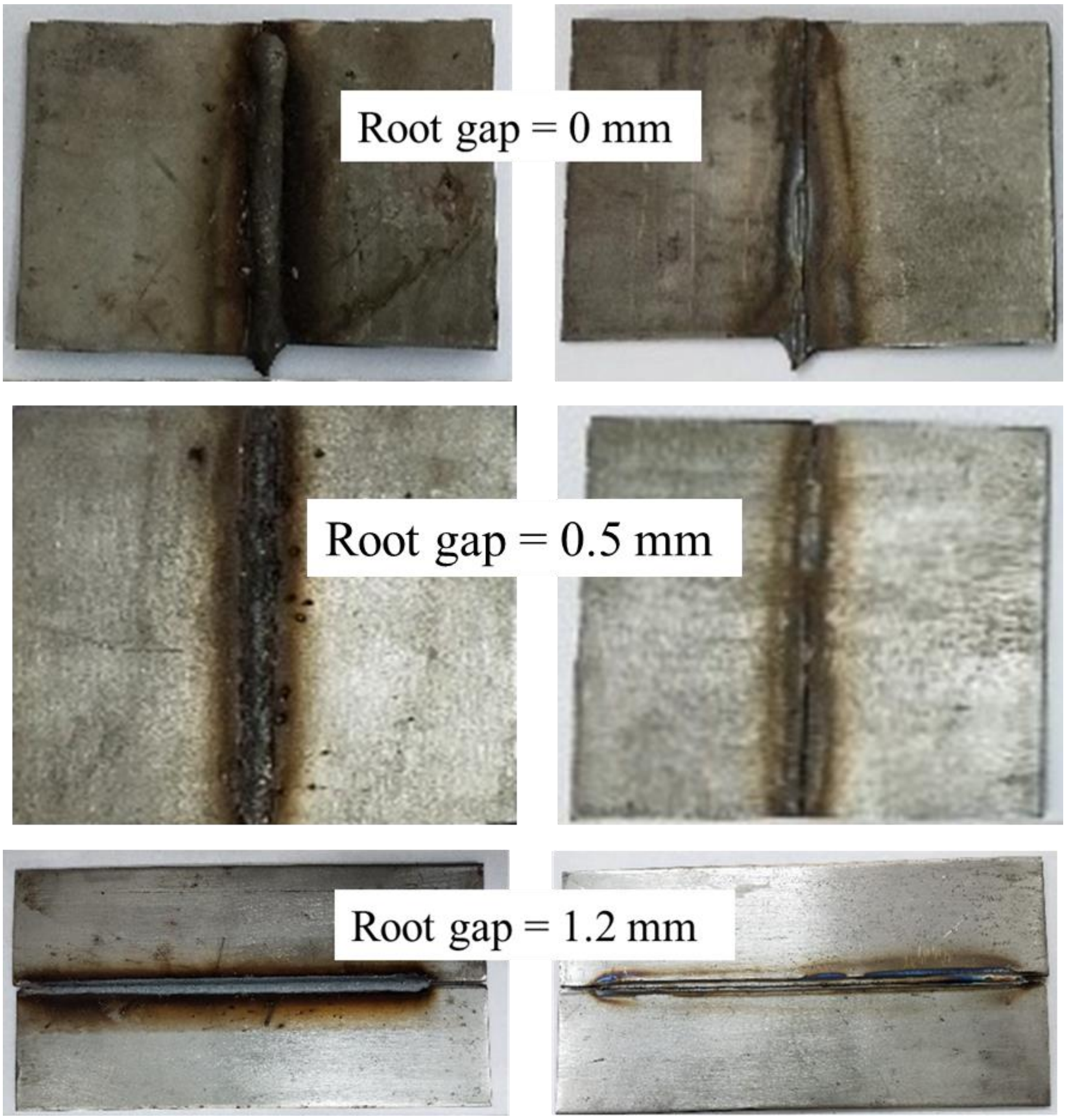

Figure 3.9 Trial runs with different root gaps.

Initially, the trial runs have been performed without any root gap. In this case, the heat of welding did not melt the material of the interfaces of both the base metals and also, the molten filler material could not penetrate up to the bottom of the plate. Full penetration did not occur even after the heat input was increased. (by using different combinations of welding process parameters), Therefore, the welding was tried using a root gap of 0.5 mm, but, in that case also, weld penetration was not complete. On further increasing the root gap up to 1.2 mm, a good weld penetration was observed. The root gap has also been shown schematically in Figure 3.10.

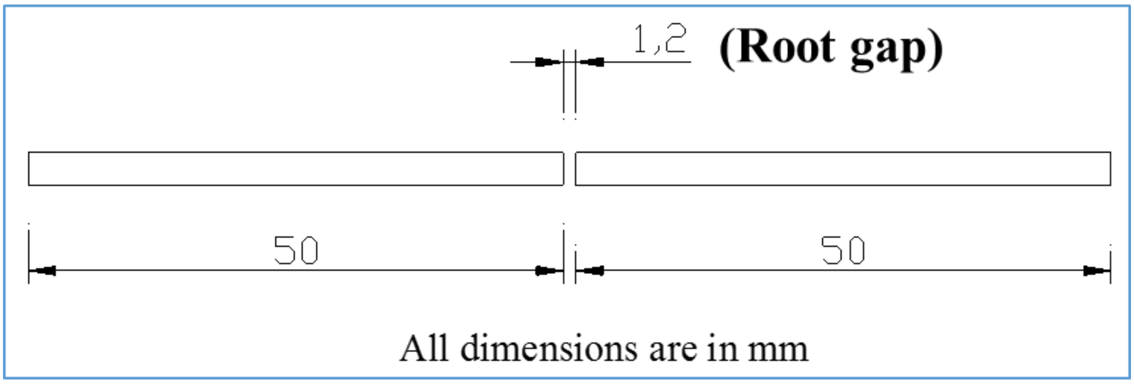

Figure 3.10 Schematic diagram of root gap.

Trial runs were also performed using a larger root gap, but a larger root gap required extra filler material, which unnecessarily increased the weight of the welded component and often caused distortion in the welded plate. Therefore the root gap of 1.2 mm was taken as the optimum root gap for the rest of the experimentation.

3.1.7.2.6 Shielding gas flow rate

The importance of the shielding gas has been described in the previous sections. Several trial runs were performed at different flow rates of the shielding gas while welding two plates. Trial runs were carried out at four different shielding gas flow rates 12, 14, 18 and 20 litre per min (LPM). The results of the bead obtained at these flow rates have been shown in Figure 3.11. Proper shielding should be provided to the molten weld pool to prevent it from surface contaminations and to avoid unfavorable gas meta reactions from taking place. To conserve the shielding gas, trial runs were carried at lower gas flow rates, and gradually, the gas flow rates were increased with each trial runs to fix the minimum quantity of gas flow rate that would produce defect-free welds. When the flow rate of the argon shielding gas was taken as 12 LPM, blowholes and porosities were observed in the weld metal, which was a clear indication of insufficient shielding gas flow rate. To eliminate these problems, the other trial run was carried out at the shielding gas flow rate of 14 LPM. From the obtained welds, it was observed that this flow rate of 14 LPM was just sufficient to overcome the issues associated with the welds when the gas flow rate was 12 LPM. To improve the weld quality further, the shielding gas flow rate was increased, and trial runs were carried out at 18 LPM as well. Good quality of weld metal was obtained with this flow rate also. On further increasing the shielding gas flow rate, i.e. 20 LPM, the same good quality of weld metal was obtained; however, this high gas flow rate caused the wastage of the shielding gases. Therefore, 18 LPM of shielding gas flow rate was found as an optimum value that gives both the weld joint's proper quality and optimum use of the shielding gas.

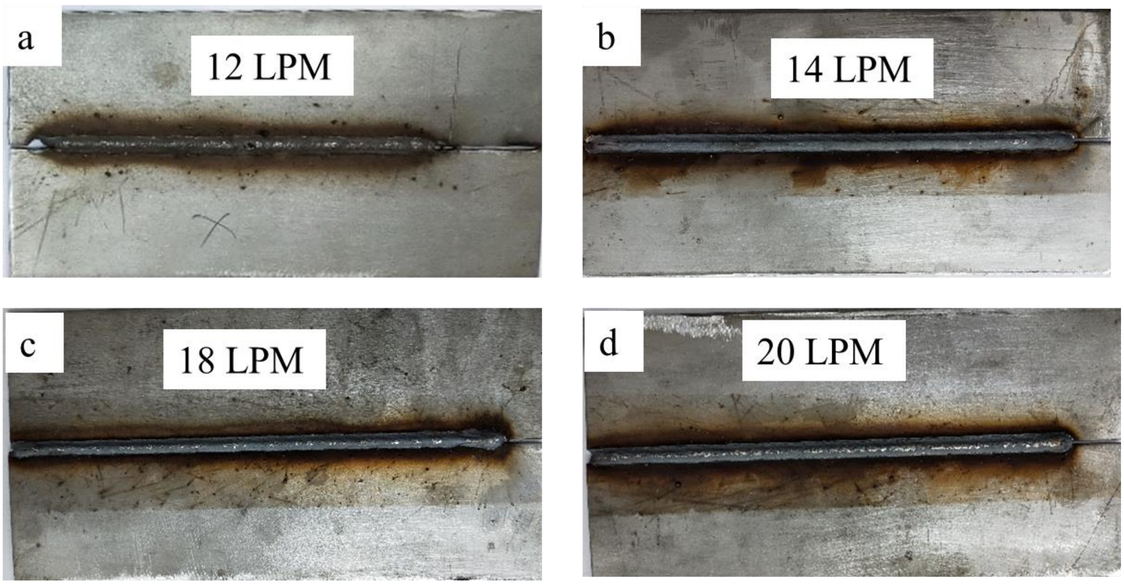

Figure 3.11 Trial runs at different rates of the shielding gas.

3.1.8 Final welding runs at the selected parameters

After welding at the selected parameters, a total of 18 samples were prepared using the ER304L electrode. The combination of process parameters used for these welding runs has been listed in Table 3.5**.** The order of experimentation was randomized to minimize the error.

Table 3.5 Different combinations of welding process parameters.

Sample	Welding current (A)	Welding voltage (V)	Weld speed (mm/min)	Heat input (J/mm)
S1	120	21	400	302.4
S2	150	21	400	378
S3	180	21	400	453.6
S4	120	24	400	345.6
S5	150	24	400	432
S6	180	24	400	518.4
S7	120	26	400	374.4
S8	150	26	400	468
S9	180	26	400	561.6
S10	120	21	500	241.92
S11	150	21	500	302.4
S12	180	21	500	362.88
S13	120	24	500	276.48
S14	150	24	500	345.6
S15	180	24	500	414.72
S16	120	26	500	299.52
S17	150	26	500	374.4
S18	180	26	500	449.28

The final welding run has been carried out at these combinations of welding process parameters. Before performing the welding runs, the plates were thoroughly cleaned with acetone. The edges of both the plates were made free of any burr that may create the problem of traversing the welding torch and proper alignment of the welding plates. The burrs were removed by using a bench grinding machine. The gas nozzle was properly cleaned periodically to ensure a supply of fresh and pure shielding gas; otherwise, contamination to the shielding gas may produce defected weld joints. The copper backing plate was also cleaned to provide a good quality of joint. In the welding process, high thermal stresses within the plates are generated, which causes the plates to distort. Therefore, to prevent unnecessary distortion, clamping of the plates should be rigid and uniform. The job clamping setup has been already described in section 3.1.6. After properly clamping the workpieces, a welding operation was carried out. The speed of the welding gun was controlled by using the knob provided on the welding trolley. Finally, successful and sound welded plates were produced at different combinations of welding process parameters.

In Table 3.5, the corresponding value of heat inputs at which these 18 samples have been prepared, is also tabulated.

Heat input per unit length of the weld was calculated from the following equation (3.1).

$$H = (\eta * V * I * 60)/WS \qquad \textbf{(3.1)}$$

Where, H is the heat input per unit length (J/mm),

η is the arc efficiency, whose value is assumed as 0.8 for GMAW process [165].

V is the welding voltage in V,

I is the welding current in A, and

WS is the welding speed in mm/min.

Using above formula, one sample for calculation of heat input is being described here. Illustrating calculation for, sample number S1,

The values of parameters are, V= 21, I= 120A, WS= 400 mm/min

On putting these values in equation 3.1

$$H = (0.8*21*120*60)/400 \text{ J/mm}$$

$$\text{Or } H = 302.4 \text{ J/mm}$$

Similarly, the heat input was calculated for the remaining samples.

Depending on the process parameters, the heat input was varying between 241.92 J/mm to 561.6 J/mm.

The photographs of a few welded plates (S4, S7 and S16) are shown in Figure 3.12.

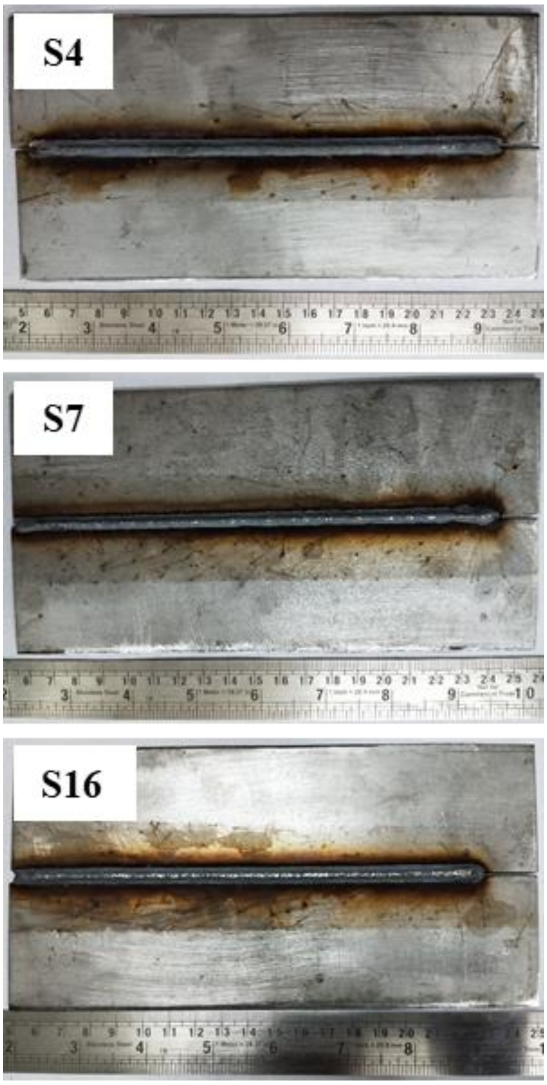

Figure 3.12 Photographs of a few welded plates obtained at different welding process parameters.

3.1.9 Characterisation of welds

To assess the quality of the welded plates, it is necessary to characterize the welded plates through various destructive and non-destructive techniques like X-ray radiography, metallographic study, hardness testing, tensile testing and Charpy impact testing.

3.1.9.1 X-ray radiography

X-ray radiography is one of the non-destructive testing technique widely used in the welding industry to detect the quality of the weld joints. X-ray radiography uses X-rays to generate the image of any internal defect present in the weld. Since X-rays can have a very small wavelength, they have a very high penetrating capability, even in metals. The penetrating capacity can be further increased by increasing the tube voltage and beam filtration. When the X-rays pass through a plate, some amount of X-rays are absorbed by the material of the plate and the remaining X-rays pass through it and can be captured by the X-ray detector placed behind the plate. The amount of X-rays absorbed depends upon the density and structure of the material. The detector may be a photographic film or a modern digital detector. When the plate possesses some discontinuity or has another material trapped inside at some locations, the amount of absorbed energy at that locations differs from the remaining locations. These variations in the absorbed energy are represented on the photographic film as the shades of black and white. Thus all the discontinuities present within the weld are easily revealed by the X-ray photographic film. A qualified technician can easily read the film and from the shades obtained, the location and type of defect can be known. However, X-ray radiography is expensive and slow technique and health hazards are also associated with it. It is recommended that well-trained person should conduct this testing. Since GMAW is a fusion welding process, which generates a large amount of heat, defects in the form of porosities, blowholes, cracks, slag inclusions, etc., are very common. Therefore X-ray radiography test is necessary to detect these flaws that are likely to be present within the weld metal.

X-ray radiography test of the welded plates has been carried out according to the ASME Section V – 2019 standard dealing with SWSI technique for radiographic examination of weldments [166]. Wire type penetrameter of DIN 10 ISO 16 FE were used to check the quality of the achieved radiograph. The image of the radiograph was captured on X-ray film (Kodak D4) with the dimensions 3″×12″. The temperature of the film was 20° Celsius. The film was developed within 5 mins. The scanned image of the X-ray film is shown in Figure 3.13. The X-ray films were shown to qualified professionals to correctly check for the nature and type of defects present in the welds. The sample image of one such radiographic films is shown in Figure 3.13. All the welded samples passed the radiography test.

Figure 3.13 X-ray radiography of welded plate.

3.1.9.2 Specimen extraction location from welded plates

Different specimens such as metallographic samples for microstructural study (denoted by M) and hardness measurement (denoted by H), transverse tensile testing (denoted by T_1), reduced section tensile testing (denoted by T_2), and Charpy impact testing specimens from WMZ (denoted by I_W) and from HAZ (denoted by I_H) were extracted from the welded plates for characterizing the welded plates.

Figure 3.14 shows the schematic diagram of the locations of different specimens extracted from the welded plates. 'D' represents the discarded material from both ends of the welded plates.

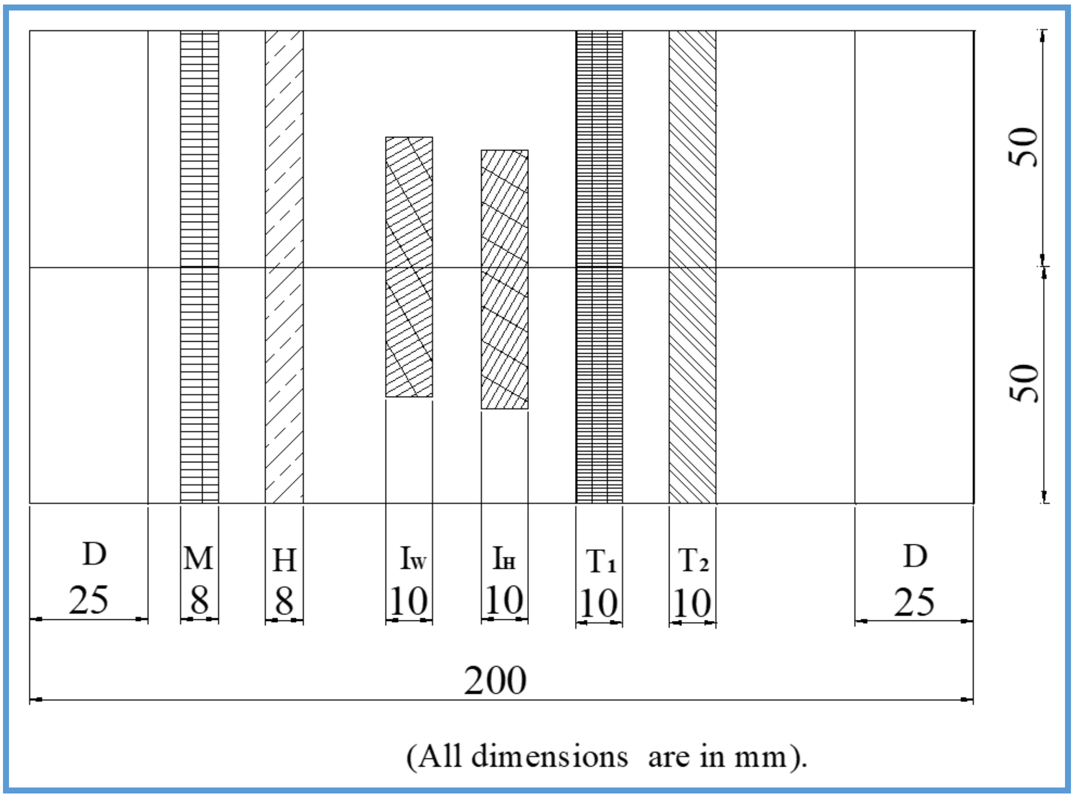

Figure 3.14 Schematic diagram of extraction of different specimens for characterisations from the welded plates.

3.1.9.3 Metallographic study

To understand the development of microstructure and formation of different phases during welding, the metallographic study of the weld plate is necessary. The metallography of the sample tells about the microstructure and grain size of the weld sample and help in predicting the properties of the weldment. They can also often reveal what was wrong during welding and what improvements are required in the weld.

3.1.9.3.1 Preparation of samples for the metallographic study

To carry out the metallographic study, samples were prepared as per ASTM standard E3-11 (2017) [167]. To prepare the sample, first, the sample of 10 mm wide and 20 mm long were extracted from the welded plate by using the band saw cutter. Then, the burrs of the extracted sample were removed by the bench grinding machine. These burr-free samples were difficult to handle for polishing due to their small size since the thickness of the sample is only 3 mm. To make it holdable, the specimens were hot moulded in bakelite by using the hot moulding machine. In this process, the bakelite was used as the moulding material to make the mould durable and rigid enough so that the moulded specimen could also be used for microhardness testing. A standard moulding machine was used for preparing the moulded specimen. While moulding, the transverse section of the specimen were placed down as the specimen were to be polished to reveal the microstructure on the transverse section. The specimens were made flat on a grinding machine and kept in the moulding machine so that after moulding, the exact transverse section was exposed and available for further polishing. The moulded weld sample was polished, first on the belt grinding machine and then on different grades of emery paper such as P120, P220, P320, P400, P600, P800, P1000 and P1200 [as per ISO (International Organization for Standardization) /FEPA (Federation of European Producers of Abrasives) grit designation] were used to polish the weld samples. The numbering associated with these P grades of emery paper refers to the amount of the abrasive material that can fit per unit square inch area of the sand paper. Higher the numbering of grades of emery paper, finer will be the grit size of the abrasive particle. The metallographic samples were rotated 90° when moving from one grade of emery paper to the next. After polishing with all the emery papers, the cloth polishing was done by using the alumina paste of 1 micron grain size. In the cloth polishing, the alumina paste was spread on the round velvet cloth placed on the round backplate of the polishing machine, which can be rotated in both directions, i.e. clockwise as well as anticlockwise. The moulded weld sample was put against the cloth having alumina paste as an abrasive particle. Due to the rubbing action between the abrasive particles and the moulded weld sample, the polishing was done. After obtaining the mirror like finish, the weld sample was cleaned with water under pressure to remove all abrasive particles present on the surface of the weld plate. The samples were finally dried using an air blower and were ready for etching.

3.1.9.3.2 Etching of the sample

The etchant used for exposing the microstructure was Kalling's reagent (10 ml hydrochloric acid, 10 ml ethanol and 0.5 g cupric chloride). The samples were swabbed with freshly prepared etchant and the etching time was taken kept as 12 seconds. Etching was done at room temperature. After applying the etchant for 12 seconds, the mould samples were thoroughly cleaned with distilled water to stop the etching reaction and remove any etchant traces. The remaining water was dried with the help of an air drier. The samples were stored in a glass desiccator to protect the surface from the atmospheric contamination and reaction with the atmospheric gases.

3.1.9.3.3 Revealing the microstructures

To observe the microstructures, an optical microscope (Dewinter, Classic PL) was used to observe the microstructure. It is a trinocular transmitted and reflected polarizing microscope. Its magnification range lies between 100 to 600. A computer is attached with this microscope to capture the images. Most of the information could be gathered by capturing the micrographs at 100 x magnification. The entire weldment was scanned under the microscope, starting from the unaffected base material to the HAZ on one side, the weld metal and the HAZ and unaffected base material on the other side.

Care was also taken to look for any microscopic defects that could have been present in the weld. Characteristic images of different regions of the weldment were captured and stored.

3.1.9.3.4 Calculation of grain size

The grain size of different regions of the weldment was found by using Image J software. The images captured by the camera attached with the optical microscope were imported in the ‘bmp’ format in the Image J software. The intercept technique was used for the calculation of grain size, which is one of the simplest technique to measure the grain size. After calibrating the scale of the microstructure, 10 horizontal lines of different lengths were drawn on the micrographs. The length of the line could have been selected as the same, or each line could be of different lengths. The combined length of all the lines was noted down. The number of intersections of the grain boundary with those lines drawn was counted. If the line intersected with a triple point, then for that intersection point, the number of intersections was counted as 1.5, instead of 1.0. The average grain size of that region was calculated as equal to the sum of the total length of all the lines divided by the total number of intersections between the lines and grain boundaries. Using this procedure, the grain size of different regions was calculated.

3.1.9.3.5 Study of percentage dilution

The actual weld bead and its schematic diagram of the transverse section of the welded plate are shown in Figure 3.15 (a) and Figure 3.15 (b) respectively.

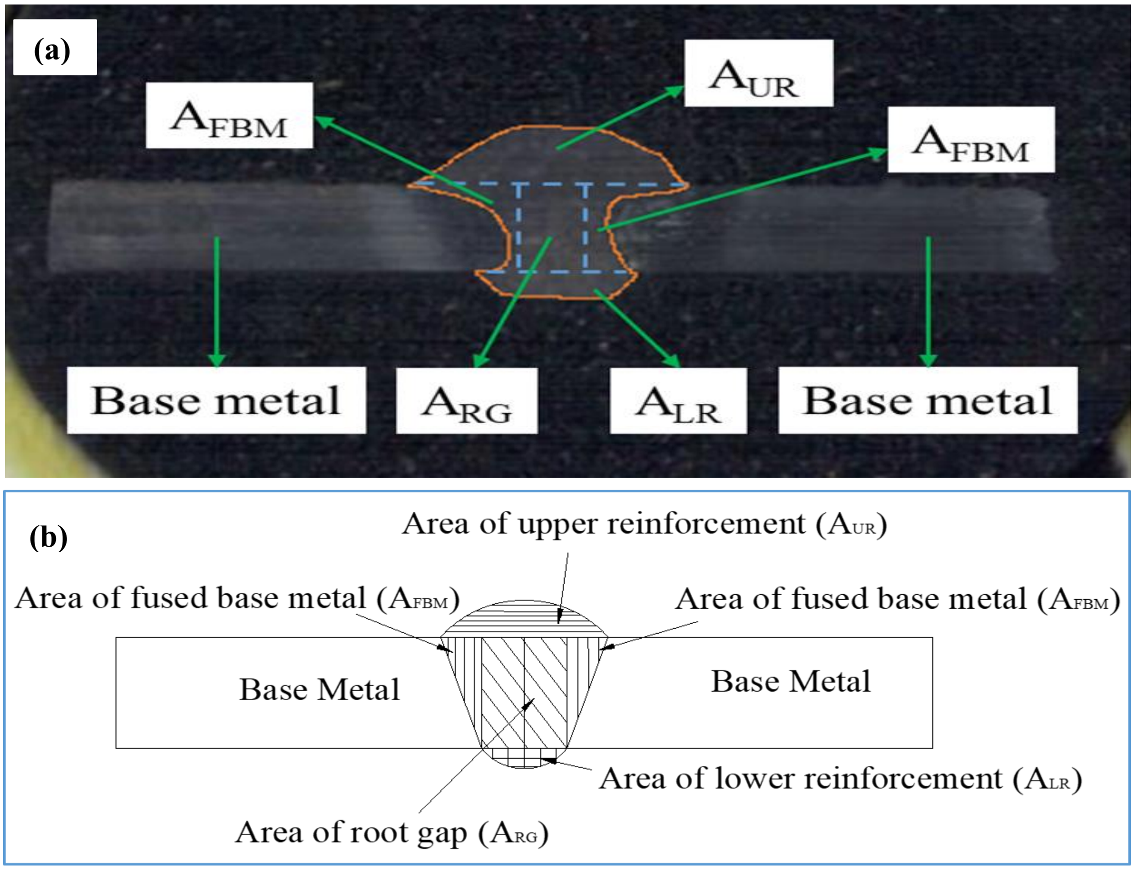

Figure 3.15 Transverse section of the welded plate (a) actual weld bead, and (b) schematic diagram.

From Figure 3.15, it can be seen that the transverse section of the welded plate consists of four distinct areas (upper reinforcement A_{UR}, lower reinforcement A_{LR}, base metal that is fused during welding A_{FBM}, and area of root gap A_{RG}). The summation of these areas is equal to the area of total weld deposition (A_{TWD}), which can be presented as shown in equation (3.2).

$$A_{TWD} = A_{FBM} + A_{LR} + A_{RG} + A_{UR} \quad \textbf{(3.2)}$$

Note, A_{FBM} is the total area of the fused base metal on both sides of the welded plate.

To find these areas, the metallographic samples of each welded plate have been prepared. The metallographic samples were scanned using a photo scanner and converted into pdf format. The pdf file of the image was opened into Adobe Acrobat Professional software and using the 'measure' tool provided in the 'more tools' option of the software, the area of the fused portion of the base material and the total area of the weld metal was measured.

Percentage dilution is the ratio of the volume of the fused base metal to the volume of total weld deposition, multiplied by 100. Since the thickness of the fused base metal and total weld deposition are equal; therefore, the percentage dilution can also be defined in other words, that, it is the ratio of the cross sectional area of the fused base metal to the area of total weld deposition, multiplied by 100, as shown in equation (3.3).

$$PD = [\frac{A_{FBM}}{A_{TWD}}] \times 100 \qquad \textbf{(3.3)}$$

Where - A_{TWD} is the area of total weld deposition, and

- PD is the percentage dilution.

After calculating the percentage dilution, the chemical composition of the WMZ has also been calculated by using the equation (3.4).

$$C(\mathbf{x})_{WM} = [\frac{PD}{100}] \times C(x)_{BM} + \left(1 - \frac{PD}{100}\right) \times C(x)_{FM} \qquad \textbf{(3.4)}$$

Where, -$C(x)_{WM}$ is the concentration of each element (x) in the weld metal,

-$C(x)_{BM}$ and $C(x)_{FM}$ is the concentration of that element in base metal and filler wire, respectively.

The concentration of each element (x) in the weld metal as calculated by equation (3.4) is merely an estimate, obtained from the chemical compositions and dilutions.

Possible pick-up reactions like gas metal reaction or element loss due to vaporization during welding have not been considered in this equation.

3.1.9.4 Hardness testing

The procedure of sample preparation for hardness testing is the same as that of metallographic study. The hardness testing has been carried out to study the average hardness of different regions like BMZ, HAZ and WMZ. The zones obtained are very thin; therefore, microhardness technique was selected for the measurement of hardness. Since the microhardness of each phase is different and each region possess different types of phases, several indentations were taken in each region. The average value of hardness obtained from these indentations gave the average of the hardness of all the phases present within that region reflecting the average hardness of that region. The Vickers microhardness was measured on the samples using the Vickers microhardness tester (SIEMENS, serial no. 104 machine). This microhardness tester machine was equipped with the facility of taking the image of the indentation as well. The location of the indentation and the gap between two indentations can be programmed in this machine. The compressive load can be varied from 10 gram to 1000 gram depending on the material being tested. The machine is also equipped with three different types of indenters to measure the Vickers hardness, Knoop hardness and Brinell hardness. Since the material used in this study was ferritic stainless steel, an appropriate load of 100 gram was used. The dwell time selected for the load being applied was 10 seconds. The machine automatically controlled the rate of loading and unloading. Hardness testing has been carried out on transverse section of the weld metal as per the schematic, as shown in Figure 3.16.

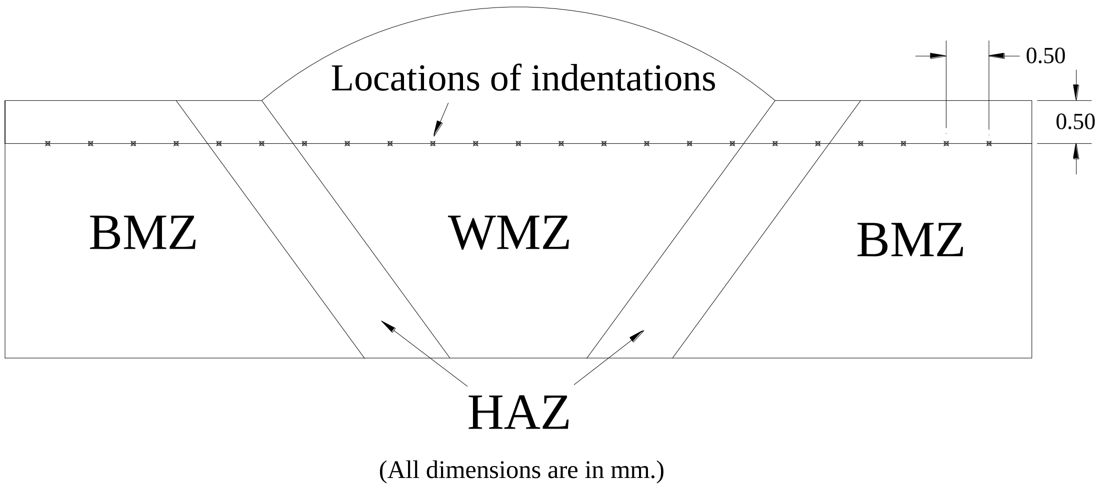

Figure 3.16 Schematic diagram of locations for hardness measurement.

The gap between the two indentations for hardness measurement in each region was taken as 0.50 mm, as shown in the above figure. It ensured a sufficient gap between two indentations, and the effect of plastic deformation of one indentation was not affecting the hardness of the next indentation. Similarly, care was also taken that the indentations maintained a gap of at least 5 times the diagonal of indentation from the free surface. Therefore, the line along which the indentations were made was 0.5 mm below the top surface of the sample.

3.1.9.5 Tensile testing

To evaluate the tensile strength of the welded component, a tensile test has been performed. Various types of tensile samples are being used for the tensile properties of the weldment, such as transverse tensile test sample, all weld tensile testing samples, and reduced section transverse test tensile sample. As per ASTM E-8 M, the tensile test specimen can be of two types [168]. The flat tensile test samples are easy to make when material is available in sheet or plate form and the round tensile test specimen that can be made if the material is available in bulk form. Both the types of specimens are prevalent in research, have their own advantages and disadvantages, and the type of specimen selected for testing is generally based on the ease of manufacturability. In this study, the welded plates were very thin, and flat specimens could be easily prepared and tested.

The transverse tensile sample is used to find the region or location within the weldment which possesses the lowest mechanical strength, i.e. the weakest region of the welded component. It also tells the strength of the weakest region of the weldment. This information is very useful for the designer as it decides the maximum load that the weldment can bear before failure. However, if the weakest region is not the weld metal, this test will not tell any information about the strength of the weld metal. In such a case, to find the strength of the weld metal, the reduced section transverse tensile sample is used. The sample for the reduced section tensile test is also machined from the transverse section of the weldment, but its width is deliberately reduced at the section, whose strength is to be found out. The width of the specimen should be sufficiently reduced to ensure that the specimen fractures in the region of interest during tensile testing. The load at failure, when divided with the reduced cross sectional area of the specimen, gives an estimate of the strength of the material in that region.

In this study, two types of tensile sample (transverse tensile sample and reduced section transverse tensile sample) have been prepared. To prepare both types of tensile samples, strips were taken out from the welded plates after the weld reinforcement have been completely removed on a shaper machine to make it flat. Since the plates were only 3 mm thick, sub-size tensile test specimens, as mentioned in ASTM-E8 standard were prepared on a CNC milling machine. Similarly, from the strips taken out from the welded plates, reduced section specimen were also prepared on the CNC vertical milling machine. The use of the CNC machine ensured accurate dimension of all the specimen with a good surface finish. The dimensions of the subsize specimen of both types of tensile samples are shown in Figure 3.17 and Figure 3.18.

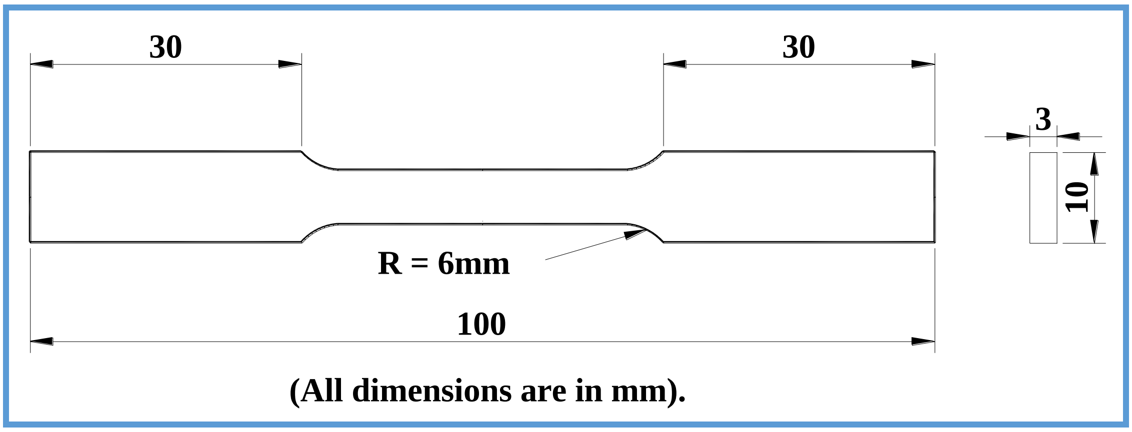

Figure 3.17 Schematic diagram of transverse tensile sample.

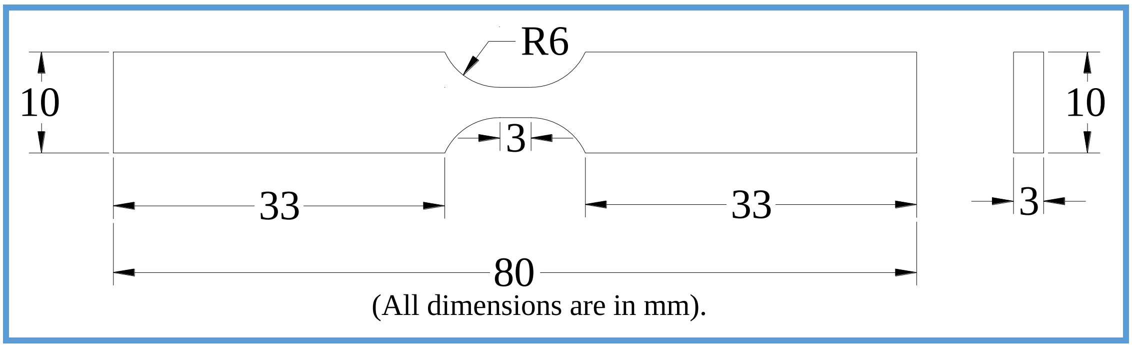

Figure 3.18 Schematic diagram of reduced section transverse tensile sample.

The different steps for making the tensile test samples and performing the tensile testing have been shown in Figure 3.19.

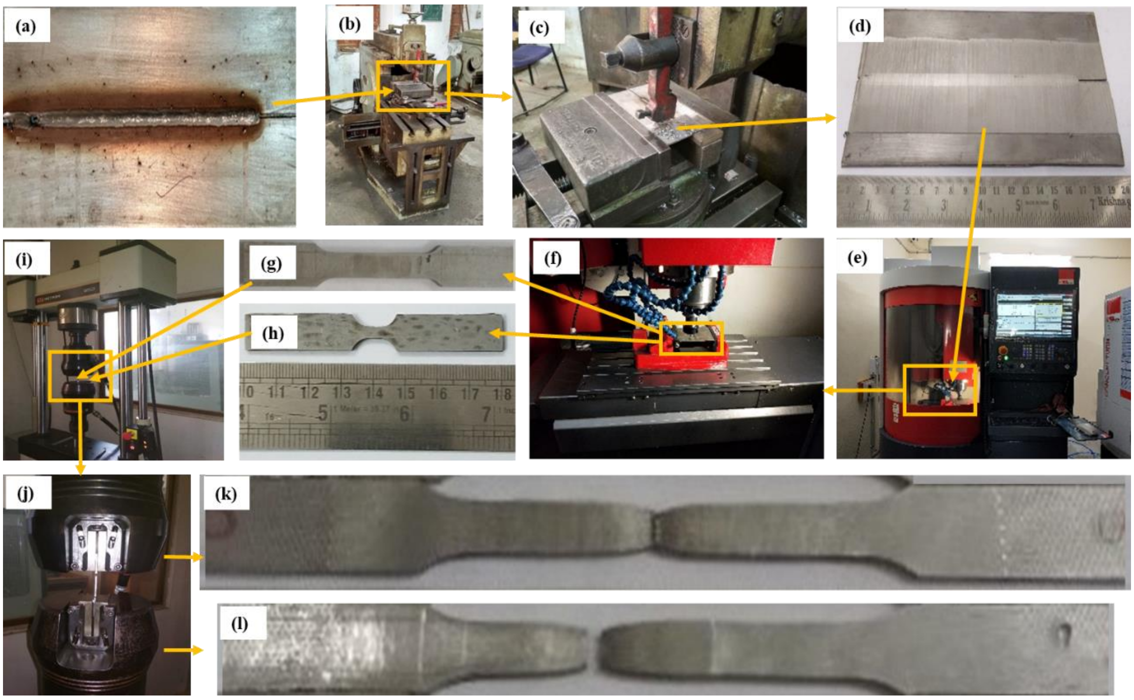

Figure 3.19 Steps followed to tensile sample preparation and performing the tensile testing operation.

(a)gas metal arc welded plate, (b) shaper machine, (c) magnified view of shaping operation, (d) reinforcement is removed to obtain flat surface, (e) CNC machine, (f) magnified view of machining operation by CNC machine, (g) prepared transverse tensile sample, (h) reduced section tensile sample, (i) universal tensile testing machine, (j) magnified view of job located within the clamps, (k) fractured base metal tensile sample after performing testing and (d) fractured welded tensile sample after performing testing.

The tensile testing has been carried out using the Instron 5982 tensile tester machine. In this machine, the grip section of the tensile sample was clamped between the jaws. The griping of the specimen in jaws was controlled by hydraulic pressure. The elongation rate of the sample was kept constant at 6 mm/min. On increasing the elongation, sufficient stress was developed in the strength, and the elongation was kept on increasing till the specimen yielded and finally got fractured. The data of the variation of stress with respect to strain was platted to find the various components of tensile testing, i.e. yield strength, ultimate tensile strength and percentage elongation. To find the yield strength, a 0.2% offset method was used since the yield point phenomenon as seen in carbon steels was not seen in the material.

3.1.9.6 Charpy impact testing

Many times, a ductile material may fail in the brittle manner in certain situations. Tri-axial state of stress, low temperature and high strain rate are the factors that contribute to the brittle failure of ductile material. The welding of material often leads to the change in this behavior of the material, and it is particularly important to test the welds in these conditions. Charpy impact testing is one method where the specimens are tested by inducing a triaxial state of stress by creating a notched specimen, and the notched specimen is fractured by loading at under impact load (to ensure a very high strain rate). The results of the Charpy impact test in terms of the energy absorbed is a good indicator of the toughness since toughness is defined as the ability of a material to absorb energy during fracture. The specimens for the Charpy impact test were also taken out from the transverse direction, and the dimensions of the sample were according to the ASTM standard A370 [169]. The photograph of one such specimen and the schematic diagram has been shown in Figure 3.20**.**

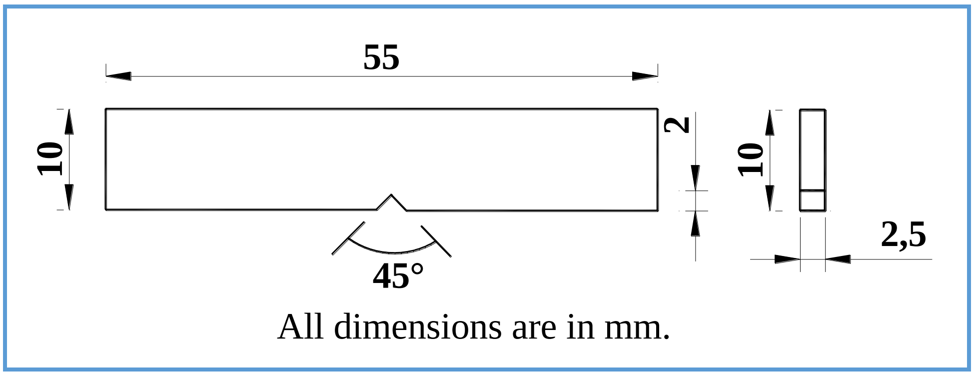

Figure 3.20 Schematic diagram of Charpy impact testing sample.

The sample was extracted from the welded plate, and the dimensions of the extracted sample were kept more than the required dimension to provide for the machining allowance. The impact sample was prepared by using the CNC milling machine.

The Charpy impact testing of the prepared samples was performed by using a pendulum type impact testing machine, as shown in Figure 3.21.

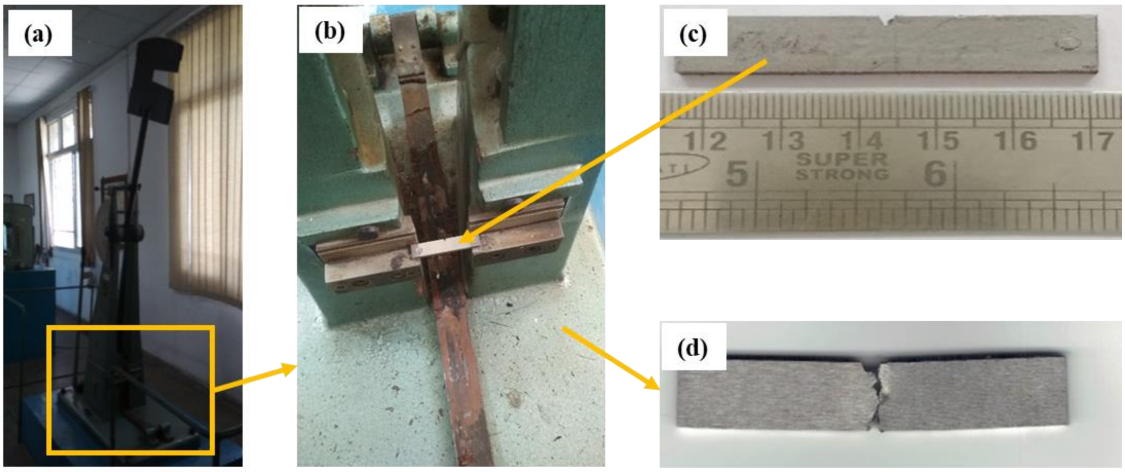

Figure 3.21 Charpy impact testing process: (a) testing machine, (b) magnified view of the sample holding location, (c) testing sample and (d) fractured sample after performing testing.

During impact testing, the sample was kept on the anvil with the notch precisely in the centre. The striking hammer is placed at a certain height from the workpiece sample. On releasing this hammer, it strikes with the sample and the sample got fractured. The hammer, after striking with the sample, loses some amount of its kinetic energy. Due to which the height obtained by the striking hammer becomes lower than the original height. The dial indicator indicates this loss in energy which is toughness of the material. The Charpy impact testing of the base metal, HAZ and WMZ has been carried out.

3.1.9.7 Residual stress measurement of the weldment

The longitudinal residual stress in each region of the welded plate S7 has been found by using the 'Stresstech Group's Xstress 3000' machine. The locations on the welded plate at which the measurement has been taken is shown schematically in Figure 3.22.

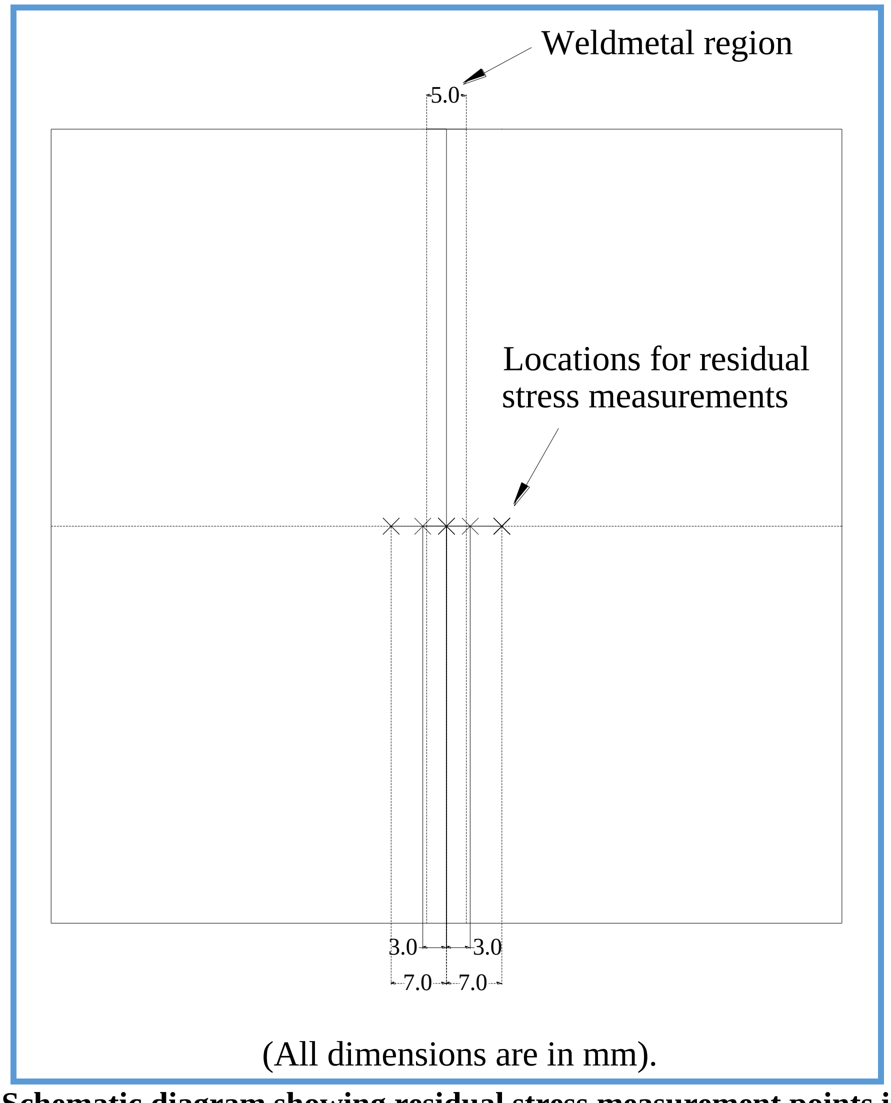

Figure 3.22 Schematic diagram showing residual stress measurement points in the welded plates.

The longitudinal residual stresses have been measured across the width of the welded plate.

3.1.9.8 Micro-magnetic characterisation of welds

To assess the quality of the welded samples of the ferromagnetic materials (such as SS409L), the testing methods based on magnetic measurements such as MBN and MHL are frequently used. Both MBN and MHL are inter-related because the strongest Barkhausen effect occurs at the coercive point of the MHLs. The MHLs are generated due to the energy loss in one complete cycle of magnetization and demagnetization of the ferromagnetic material placed under the constant varying magnetic field. Both MBN and MHL are widely used for the characterisation of ferromagnetic materials. MBN technique is one of the widely used non-destructive testing techniques for microstructural and stress analysis of ferromagnetic material [170-178]. It is a portable, less time-consuming and less costly than other laboratory-based techniques such as X-ray diffraction (XRD) and metallographic study [170, 179]. Various parameters like RMS value, peak value, spectral density and number of pulses are used to analyze the MBN signal [180, 181]. Various researchers have investigated the relationship between these MBN parameters with the grain size, microhardness, residual stress, applied stress and the C content of the material.

The characterisation of different zones of weldment (WMZ, HAZ and BMZ) of sample S7 has been done by the MBN technique. The present work consists of a detailed investigation about the variation of MBN activity with the grain size of different zones as well as the variation of MBN activity with the variation of magnetizing frequency and magnetic field intensity (MFI).

The samples of proper dimension were cut for carrying out MBN analysis as well as MHL analysis. For sample preparation to carry out analysis, reinforcement of welded plate was removed up to the surface of the BM by shaping operation because pickup sensor requires an almost flat surface to catch the voltage change in the coil due to movement of magnetic domain walls. The surface was smoothened further by using emery paper. MBN measurement was carried out on the surface of the BMZ, HAZ and WMZ of the welded plate by using Magstar MBN analyzer (jointly manufactured by Technofour, Pune and National Metallurgical Laboratory, Jamshedpur, India), which is shown in Figure 3.23. For a better understanding of the machine setup, it is also shown schematically in Figure 3.24.

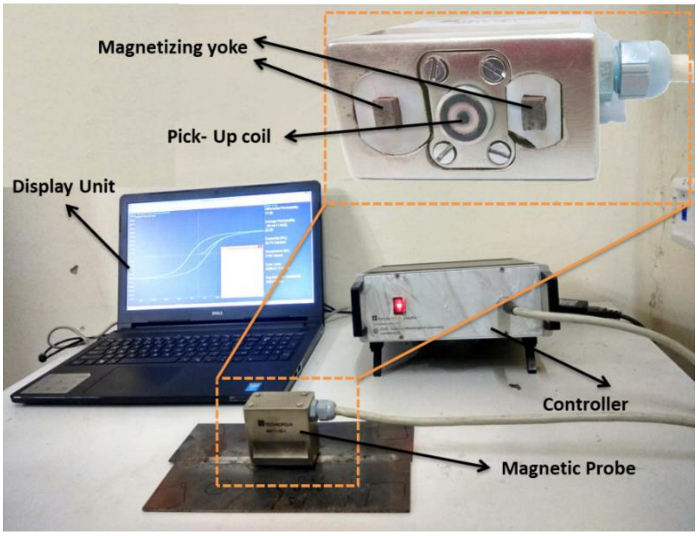

Figure 3.23 MBN analyser setup.

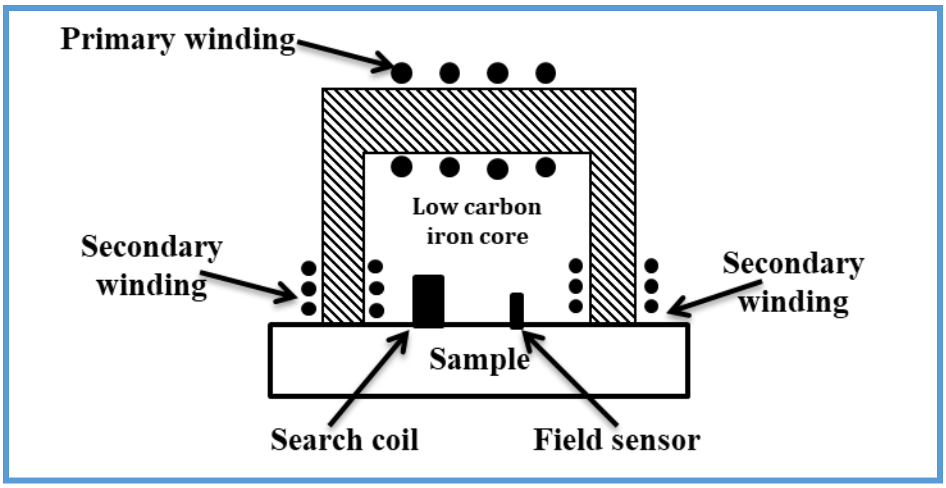

Figure 3.24 Schematic diagram of MBN analyser.

MBN setup consists of mainly two components, one is a flat surface probe, and the other is a display unit. The flat surface probe comprises two parts: U-shaped yoke, and the other is a pickup sensor used to generate the varying magnetic field and receive the MBN signals, respectively. The pickup sensor, which is located in the centre of the probe, consists of a sensing coil wrapped on a movable soft ferrite core of high permeability, which is pressed over the examined surface by spring force to maintain contact.

To perform MBN operation, the magnetic field was applied at different zones of the welded plate (BMZ, HAZ and WMZ) at four different magnetizing frequencies (10, 20, 30 and 40 Hz) with a constant MFI of 800 Oe as well as at five different MFI (250, 500, 750, 1000 and 1250 Oe) with constant magnetizing frequencies of 25 Hz. The generated raw MBN signal was captured by pickup sensor, and due to the high permeability of ferrite core, magnetic amplification of raw MBN signal was done. The amplified signals were filtered using a 100–300 kHz band-pass filter to eliminate low-frequency interferences and high-frequency harmonics. The filtered, amplified MBN signal was displayed on the display unit along with the analysis of the signal. The analysis of the signal was carried out in terms of two parameters: V_{rms} and the number of pulses. While to perform MHL operation, five levels of magnetising frequency (0.05, 0.10, 0.15, 0.20 and 0.25 Hz) was taken in low frequency range, and four levels of magnetizing frequency (1.0, 2.0, 3.0 and 4.0 Hz) was taken in high-frequency range at a constant value of magnetic field intensity (800 Oe). Test has been performed repetitively at different locations, and it was found that variation in the values was within 2 percent. Finally, one location was selected to carry out the test. Magstar and Origin pro software further analyzed the signals.

Part – II

3.2 Friction stir processing of gas metal arc welded ferritic stainless steel

3.2.1 Introduction

Grain coarsening in the HAZ of ferritic stainless steel is a major drawback, which cause the reduction in the mechanical properties of the welded joints. Friction stir processing is a technique which can refine these coarser grains in order to improve the mechanical properties.

In all of the welded plates, it was found that the HAZ possessed lower hardness than the BMZ and WMZ. All the transverse tensile test specimen also fractured in the HAZ which clearly indicate that the HAZ was the weakest zone of the weldment. The reason for low hardness and poor tensile strength was due to the large size of grains that were present in the HAZ when compared with the size of the grains that were present in the base material or the WMZ. To refine these coarse grains of the HAZ and consequently to improve the mechanical properties of the welded plate, FSP operation has been carried out on the welded plate. The minimum grain size that could be achieved in any HAZ was found to be present in samples that were welded as per the parameters corresponding to sample S7 (however, the grain size in HAZ of sample 7 was still coarser than that of the base material and the weld metal). This less coarse grained structure has therefore led to slightly superior mechanical properties of sample S7. The sample S7 is selected because out of all the welded samples, the sample S7 possess the highest value of tensile strength (UTS 399 MPa, YS 260 MPa). Impact strength and hardness of the heat affected zone of sample S7 was also found to be higher than the other welded samples. Therefore, to improve mechanical properties further by refining the heat affected zone as well as weld metal region, the sample S7 has been selected for carrying out friction stir processing upon them.

In this section, the process of carrying out the FSP of the welded plate S7 has been elaborated step by step. First, the FSW machine is introduced, and then the selection of the FSP tool material is described. The selection of the tool profile and how the tool of a given profile is produced by using a tool grinder machine is also described. Several trial runs have been carried out to find the window for the process parameters in which the FSP of the welded plates have been carried out successfully. After carrying out the final run with two different SDs (15 mm and 20 mm) and three different ratios of the RS to the PS (6, 9 and 12 revolution per mm), the characterisations of the processed plates (metallographic study, XRD analysis, hardness testing, tensile testing and Charpy impact testing) have been carried out. The MBN and MHL analysis of the PR of sample A at constant values of MFI of 800 Oe and magnetising frequency of 0.05 Hz have been carried out. In this section, only the procedure of the experimentation and characterisation of samples have been discussed.

3.2.2 Friction stir processing equipment

FSP was carried on a FSW machine (FSW – 3T NC). The FSP machine setup which was used in this work, has been shown in Figure 3.25.

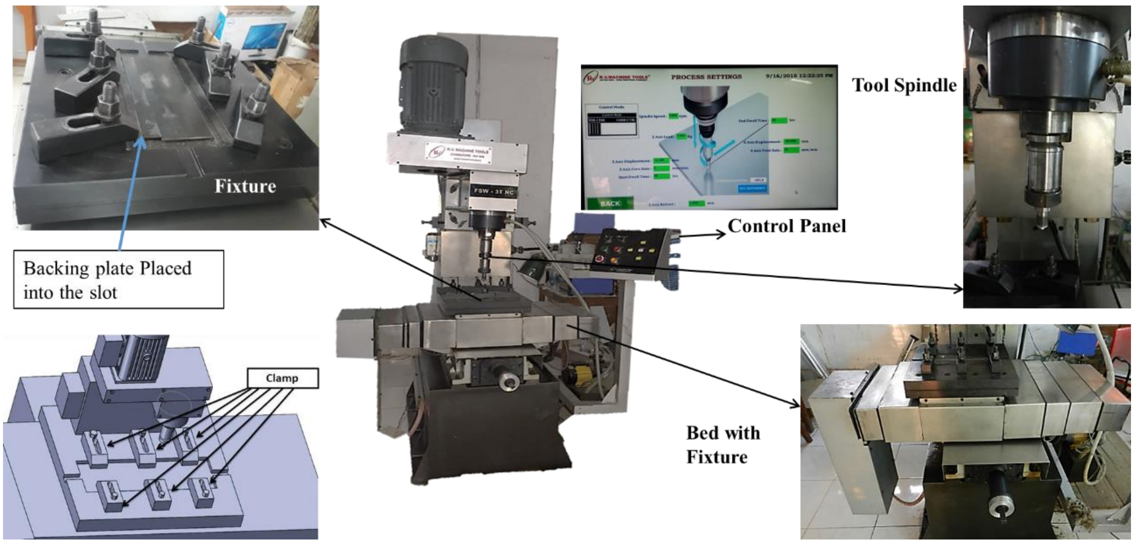

Figure 3.25 FSP machine setup.

FSW machines can usually be operated in position controlled mode or force controlled mode. In position controlled mode, the machine is operated so that the Z-position is maintained irrespective of the Z-thrust generated. In force controlled method, the Z-thrust is maintained within a particular limit. For an uneven surface, this may require a slight change from the pre-set value of the Z-position. In this study, the plate used for FSP was already made flat, and therefore, the machine was run in position controlled mode. FSP machine setup consists of clamping arrangement, computer to feed the processing parameter, tool holding setup. During the FSP, high pressure is applied by the rotating tool on the workpiece and simultaneously large amount of heat is also generated. This combination of temperature and pressure is required to perform the processing operation. To prevent the plates from moving along with the tool, the clamping of the plate must be sufficiently rigid. The machine should also be robust enough to bear this large amount of pressure, particularly during the FSP of stainless steels. The clamping setup consists of a robust backing plate, supporting the high pressure generated during the FSP operation. The welded plate was kept on this backing plate and clamped tightly to perform the FSP. In this study, the length along which the FSP is carried out corresponds to the X-axis, the width of the plate corresponds to the Y-axis, and the direction along which the tool is plunged during processing is the Z-axis. This entire clamping setup is mounted on the sliders through which the plate being processed can be moved with respect to the FSP tool along the X-direction. The slider can be moved in the Y direction to position the plates so that the region to be processed can be brought directly below the FSP tool. The centreline of the process region should lie exactly in the centre of the tool to perform the FSP operation.

The tool holding setup consists of the water cooled spindle, collet chuck (with collets of specific sizes as required for the tool). The spindle is rotated at a given RPM with the help of a 15 kW motor. The process parameters such as PS, tool RS and direction, transverse length and tool plunge (corresponding to the tool pin length and the depth up to which processing is required to be carried out). The tool geometry, notably the SD and pin length of the FSP tool, depends on the specific requirement of the process. The more the diameter of the tool, the more the area of the material will be processed. With a larger pin length, the more the depth of the material can be processed, and the depth of the PR is nearly equal to the pin length of the tool. The machine used is a CNC machine that is controlled by a computer associated with this machine in which these process parameters are set. Then, the starting and stopping of the rotation of the tool can also be controlled by the knob on the panel of the machine. In this panel, eleven different knobs for different purposes are given. These knobs are: Spindle on/off, auto on, emergency off, manual/auto, power on, servo set, rapid, Z+, Z-, X+ and X-.

During the processing operation of high temperature softening materials like stainless steel, a large amount of heat is generated, damaging the tool holder and main spindle bearing. Therefore, to prevent damage to the tool holder and main spindle bearing, proper cooling of the tool holder is necessary. A water jacket is made around the spindle bearing where the coolant is continuously circulated. The coolant mixed with freshwater is pumped by a pump (0.25 HP) to the water jacket. The excess heat reaching the spindle bearing and the tool holder is transferred to the coolant. The big sump attached to the cooling pump ensures that the warm coolant transferred to the sump is cooled before being recirculated. The wear and tear of the components of the FSP machine may also occur because the machine is heavily loaded when working on stainless steels. To protect the components of the machine, a dedicated lubrication system is there in the machine. Lubrication is done by the hand operated pump. In this pump, a lever that is operated by hand is used to pump the lubricating oils to different parts of the machine.

The complete specifications of the FSP machine (Model FSW- 3T-NC) used for the FSP experimentation are given in Table 3.6.

Table 3.6 Specification of the FSP machine.

Parameters	Rated value
Z-axis load (maximum)	3 Ton
Spindle nose	ISO 40
Spindle speed	3000 rpm
Z-axis travel	300 mm
Table to spindle	Min/Max 500 mm to 800 mm
Z-axis velocity	1000 mm/min
X-axis travel	300 mm
X-axis velocity	3000 mm/min
Range of tilt angle	±7°
Controller	Force and Position mode control
Data acquisition	Spindle rpm, torque axis velocity, force against time and distance

3.2.3 Selection of friction stir processing tool material

To perform the FSP on the welded plate, the selection of the FSP tool material is a difficult task. Since the FSP is carried at a high temperature (above the recrystallization temperature of the material), the FSP tool must maintain its strength at these high temperatures. Apart from that, it should be wear resistant and harder than the workpiece material. The FSP tool must also be non-reactive towards the workpiece material. Machinability of the FSP tool material is also considered as one of the main factors in their selection so that the FSP tool can be prepared of proper dimensions according to requirement. The selection of the tool material mainly depends upon the hardness of the workpiece material. A brief discussion about the different possible FSP tool materials are given here:

3.2.3.1 Tungsten

It is also known as wolfram, from which its symbol 'W' comes. It possesses the highest melting point (3422 °C) of all the elements known, along with the highest boiling point (5930 °C). The hardness of tungsten is very high (7.5 on Mohs scale), but at the same time, it is very brittle and difficult to machine. It offers high tensile strength and possesses the capability to retain this strength at high temperatures. Thus, tungsten is a possible FSP tool material for processing steels. The ductile to brittle transition temperature of tungsten is around 400°C, and thus, it is required to heat it up to this temperature, if it is to be used as an FSP tool. A gas welding torch is usually used to heat this material to increase the temperature of this material up to 400°C before initiating the FSP.

3.2.3.2 Tungsten-Rhenium alloy

High ductile to brittle transition (DBT) temperature of tungsten material requires preheating the tool to above 400°C by gas welding torch to use it as a FSP tool. However, the DBT temperature can be reduced by adding some amount of rhenium element as an alloying element to the tungsten material, forming Tungsten-Rhenium alloy. It became possible to reduce the ductile to brittle transition temperature to below room temperature by adding rhenium up to 25% by weight. Thus, W-Re alloy with 25% Re can be used without any requirement of preheating. The addition of rhenium also improves thermal stability and creep stability, but it also offers some disadvantages like reduction in corrosion resistance and wear resistance. Due to its poor tribological properties, the formation of wear debris of tool material during processing occurs. The introduction of these wear debris into the PR deteriorates the mechanical properties of the processed material.

3.2.3.3 Tungsten carbide

Tungsten carbide (WC) is found basically in powder form, and to manufacture any tools including the FSP tool by this material, the sintering process is used. The binder during sintering is usually cobalt or iron in varying amount. The stiffness of tungsten carbide is nearly double to that of steel, with a young's modulus nearly equal to 530–700 GPa, a bulk modulus of 630–655 GPa, and a shear modulus of 274 GPa. Due to these high values of young's modulus, bulk modulus and shear modulus, this material is able to maintain its shape under extreme conditions of load applied. It also possesses high tensile strength and a high hardness of about 9 to 9.5 on the Mohs scale. The melting point of WC is 2,870 °C, and the boiling point is 6,000 °C which indicates its high refractoriness properties. It also possesses a low coefficient of thermal expansion, which is beneficial for high temperature applications. Depending on the amount of binder present, it can possess high impact strength even at low temperatures to sustain some impact loads during the processing of rough surfaces. Tribological properties and corrosion properties of this material are appropriate, so the problem of introducing wear debris into PR (as may occur in tungsten - rhenium alloy) is eliminated, which results in improved quality of the processed material. To perform the FSP process, heat treatment of this material is also not required.

3.2.3.4 Polycrystalline cubic boron nitride

In the term of hardness, the hardness of polycrystalline cubic boron nitride (PCBN) just is one step lower than that of diamond, which is the hardest material on the earth. PCBN is made up of boron and nitrogen, having a polycrystalline structure. The powder metallurgy process is used to manufacture this material, which increases its hardness to an extreme level. In the making of PCBN, some materials like copper, nickel, TiC, TiN and alumina are used as binding materials. PCBN offers unparalleled performance in terms of hot hardness, toughness and chemical stability, along with excellent tribological properties. Due to these excellent properties possessed by the PCBN material, it is one of the most suitable material to use as FSP tool material when processing stainless steel. PCBN can not be used in this work because of its high cost and difficulty in fabricating it into the FSP tool. However, a much cheaper material, WC has been used to produces defect free processing during this work.

3.2.4 Tool grinder

The tool grinder with the details of fixing the WC rod is shown in Figure 3.26.

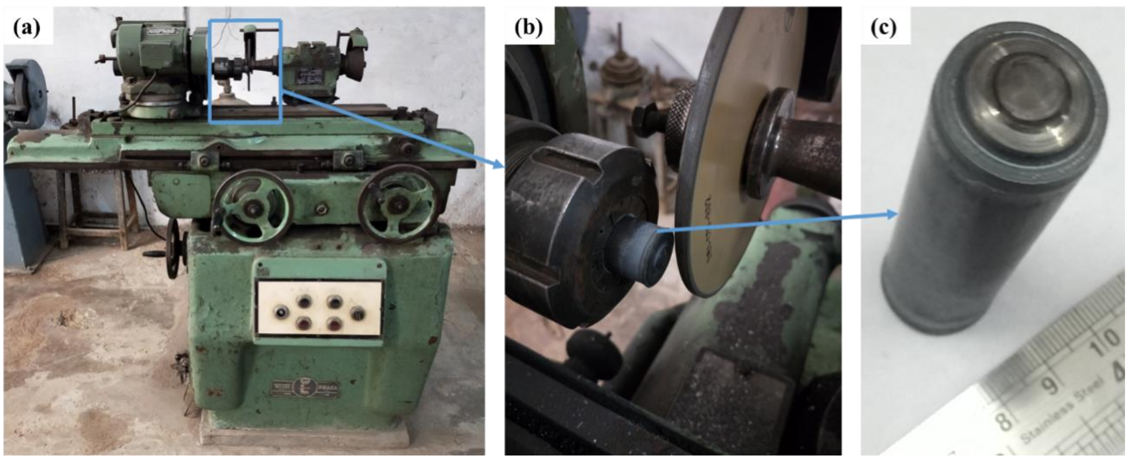

Figure 3.26 Photographs of FSP tool profile preparation (a) tool grinding machine, (b) closure view of tool and grinding wheel, and (c) prepared FSP tool.

To generate the proper tool profile, the outside diameter grinding process was used. An outside diameter grinding machine (machine no. 1912, manufactured from PRAGA TOOLS LIMITED, Secunderabad) installed in the laboratory, was used to produce FSP tools of required tool geometry.

Since WC is a very hard material, the diamond grinding wheel was used for its grinding. The grinding wheel (150 mm outer diameter, 25 mm inner diameter and 10 mm width) was mounted on the wheel head, and the WC tool material (20 mm diameter) in the form of a bar was mounted on the workhead by using a collet chuck. Both grinding wheel and FSP tool material can rotate about their axis. The workhead was mounted on the sliding table, which facilitates the longitudinal motion to the FSP tool. Transverse motion between the FSP tool and grinding wheel was carried out by moving the wheel head. Both longitudinal and transverse motions were carefully done manually by using table traverse handwheel and crossfeed handwheel, respectively. An arrangement of taper grinding is also provided in this machine. According to the requirement, the workhead and wheel head can be swivelled from 0 degree to 180 degree. Thus, it provides the facility to generate several types of profile, like tool with flat shoulder, the tool with concave shoulder, the tool with taper pin, the tool with the straight cylindrical pin, and tool with the stepped pin.

3.2.5 Selection of tool profile

Selection of the shape of the tool profiles generally depends upon the workpiece material to be processed. For an unknown material, tool profiles are optimized. The tool with straight cylindrical pin and tool with taper pin are two different types of tool pin profile that are easier to produce than the other types. In this study, several trial runs have been carried out using both types of tool profiles. On the one hand, the tool with a straight cylindrical pin produces defective plates; on the other hand, the tool with a taper pin produced a good quality of processed plates. Therefore, the FSP tool with a taper pin profile was selected for the current study.

3.2.6 Processing trial runs on gas metal arc welded plate

Trial runs were performed to investigate the range of process parameters like PS, RPM of tool and tool tilt angle in which successful processing of welded plates could be carried out. Both the base material and welded plate were used for the trial runs. To perform the FSP operation, firstly, the reinforcement of the welded plate was removed by the shaper machine and then the FSP operation is performed on the welded plate, as shown in Figure 3.27.

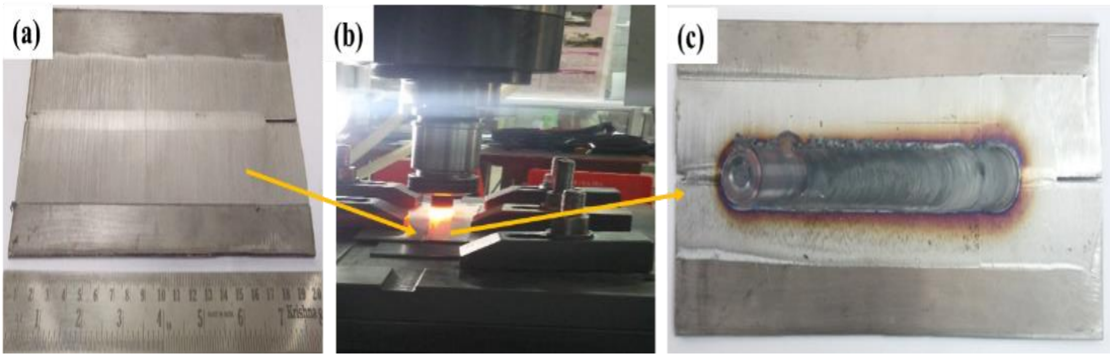

Figure 3.27 Photographs of the sequence of FSP of the welded plate: (a) welded plate after shaping operation, (b) performing FSP operation on the welded plate, and (c) FSPed welded plate.

Several factors such as the inaccurate amount of shoulder plunge and insufficient amount of clamping forces have been found during the trial runs, leading to the generation of several defects during the FSP operation. These defects were eliminated before going to the final experimentation.

Extensive trial runs were carried out by varying one parameter at a time to find the range of process parameters that could be varied and the parameters that were to be kept fixed during FSP experimentations. The details of these trial runs have been given below.

3.2.6.1 Processing speed

The speed at which the FSP tool travels between two endpoints in the interested region during FSP operation is known as processing speed (PS). Higher the PS, lower would be the heat distributed per unit length to the material being processed. The PS should be as high as possible. However, too high a PS may lead to improper flow of material, and defects may occur. It would also put tremendous stress on the tool material, if the work material has not been heated and softened up and may lead to tool breakage. Too low PS would not only lead to poor productivity, but unnecessary heating of material can also affect the properties of the PR. Therefore it is necessary to find out the maximum PS which can perform FSP operation successfully. It is also required to know the minimum limit of PS because very low PS may lead to the high amount of heat generation on the plate. This high amount of heat may damage the tool as well as the plate to be processed. Therefore, to perform the FSP operation successfully, the range of PS should be determined.

After performing several trial runs, the range of PS should lie from 100 to 140 m/min.

3.2.6.2 Tool rotational speed

Rotational speed (RS) of the FSP tool has a direct impact on the generation of heat in the FSP operation. As the RS of the tool increases, due to more friction between the tool and the plate, the generation of heat increases. The high amount of heat generation may damage the tool as well as the plate. Whereas, if the RS of the tool is much lower, then also FSP operation cannot be performed due to insufficient amount of heat generated. Therefore, the range of the RS of the tool must be found to perform the

FSP operation successfully. After carrying out various trial runs, 800 to 1200 RPM has been found as the range of tool RS.

3.2.6.3 Tool tilt angle

It is the angle between the axis of the tool and the direction normal to the base plate to be processed. The tool is tilted slightly on the trailing side during FSW and FSP to maintain proper contact between the trailing side of the shoulder and the material. It facilitates the proper flow of plasticized material and consolidation of the material behind the moving tool. Tool tilt angle depends upon the material being processed. Improper tool tilt can lead to the formation of shoulder void and other defects. Therefore, the correct tool tilt angle should be found to perform FSP operation successfully. Several values of tool tilts were tried, and it was found that a tool tilt of 1.5° produced defect free FSP. Therefore, throughout all the experimentations, the tool tilt was fixed as 1.5°.

3.2.6.4 Inaccurate amount of insertion of tool pin

During the FSP operation, the shoulder of the tool must be in proper contact with the material, and the shoulder can make proper contact only when the tool pin has properly inserted into the material. Theoretically, the length of the pin should be equal to the required depth up to which the material should be processed, but practically it is not so because to make the proper flow of the material, the shoulder must be inserted to a limit which is known as shoulder depression. The practical problem arises to investigate the proper amount of shoulder depression.

When the tool pin is not inserted sufficiently to make proper contact of the shoulder with the plate or, in other words, when the shoulder depression is less, the material cannot flow, leaving a circular impression on the material plate. On the other hand, when the insertion of the tool pin into the material is more than required, the large amount of shoulder depression will cause the flow of plasticized material in a very large quantity, which is also not good. Therefore it is always required to ensure the proper amount of tool insertion to make the proper flow of plasticized material.

3.2.6.5 Insufficient amount of clamping forces

During FSP operation, due to the rotation of the tool at very high RPM, a large amount of torque is produced, and if the clamping force is not sufficient during FSP operation, the vibration produced due to the large amount of torque may deflect the FSP tool from its location. If the tool gets deflected from its central position, the formation of ripples will not be uniform that will deteriorate the mechanical properties of the processed plate. Hence, a proper clamping arrangement is necessary to produce uniform ripples on the processed plate.

3.2.7 Outcome of the trial runs

After performing many trial runs, the tool profile has been optimized, and the range of process parameters has also been found.

3.2.7.1 Optimization of tool profile

Different tool profiles of different dimensions have been tried to conduct these trial runs. After going into a large number of trial runs by the hit and trial method, a tool with a flat shoulder and conical pin was obtained to carry out this experiment successfully. The FSP tool with two different SDs (15 mm and 20 mm) was selected for this study. The schematic diagram of one tool (having SD of 15 mm) with dimensions as well as actual tool are shown in Figure 3.28, in which SD represents the shoulder diameter, PL represents the pin length, LPD represents the lower pin diameter and UPD represents the upper pin diameter of the FSP tool.

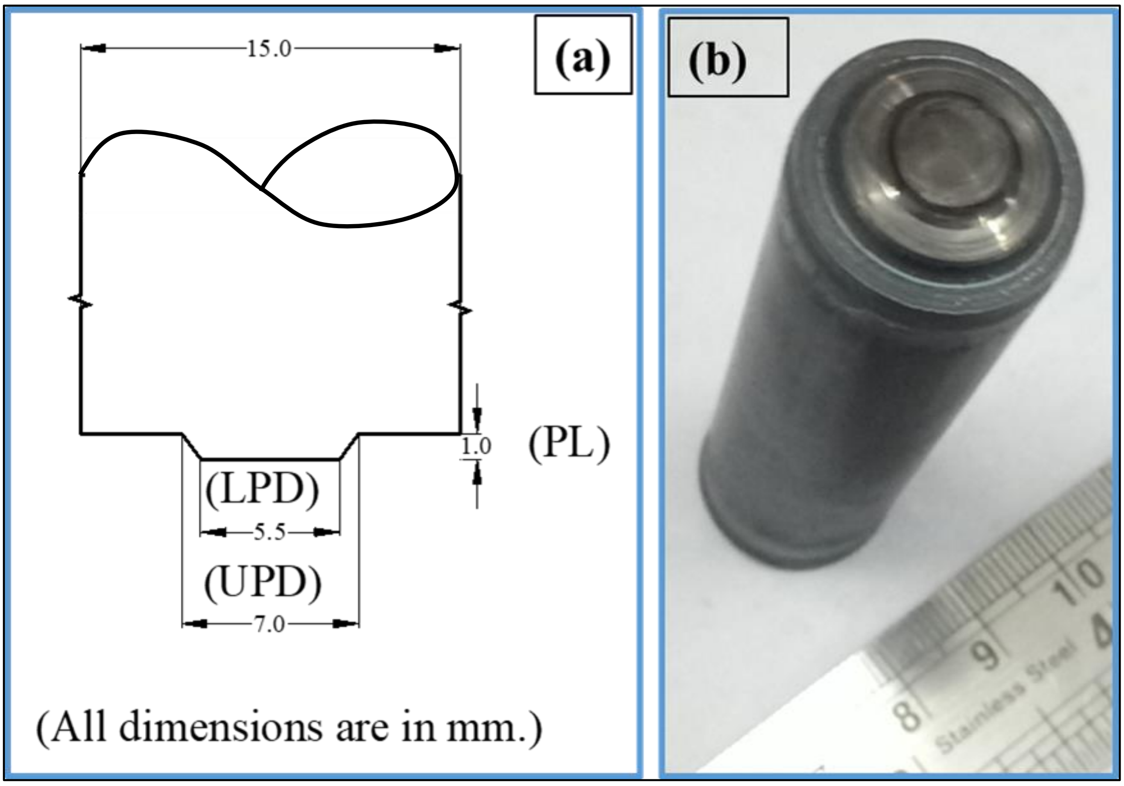

Figure 3.28 Profile of FSP tool: (a) schematic diagram of FSP tool, and (b) actual FSP tool.

3.2.8 Final runs

The heat generated during FSP operation depends upon the RS as well as the PS. A higher amount of heat will be generated for a combination of high RS and low PS, whereas a lower amount of heat will be generated for a combination of low RS and high PS. During the final run, the process parameters were selected in such a way that for a particular SD, the value of rotation per mm (RS / PS) becomes 12, 9 and 6. To study the effect of rotation per unit length on the response parameters (i.e. grain size, hardness, tensile strength, Charpy impact toughness), the ratio of the RS to PS was taken as a process parameter, rather than taking the RS and PS individually. The process parameters which were selected within the process parameters range are shown in Table 3.7.

Table 3.7 Process parameters of FSP on welded SS409L plate.

Sample	SD (mm)	RS (revolution per mm)	PS (mm per min)	RS / PS (revolution per mm)
A	15	1200	100	12
B	15	1080	120	9
C	15	840	140	6
D	20	1200	100	12
E	20	1080	120	9
F	20	840	140	6

To perform final experimentation on the welded plate, the upper reinforcement was machined by shaping operation. After that, the burrs were removed by the bench grinding machine to make them easily handable. Some extra thickness of the material (0.3 mm) has been removed by shaping operation, and the final thickness of the welded plate after shaping operation became 2.7 mm, instead of originally 3.0 mm. The plate was clamped rigidly by the clamping arrangement to prevent any plate movement during the FSP operation. The clamping arrangement consisted of total of six clamps, three at each side. After proper clamping of the plates, the process was performed.

During the FSP operation, the FSP tool's direction was from the right to the left side. At the starting point on the plate, i.e., the rotating FSP tool was plunged on the right side. The plunging speed, i.e. Z-axis velocity of the FSP tool, was kept very low (5 mm/min) to avoid any breakage of the tool pin. In the initial stage of plunging of the tool, due to the friction between the tool pin and material, frictional heat was generated, which plasticized the localized material, and made the further plunging of the tool pin into the material easier. After full penetration of the tool pin into the material, the shoulder came into contact with the material, which generated frictional heat, and the material gets further plasticized. Start dwell time (15 second) was provided to the FSP tool so that the material gets sufficiently heated and plasticized to make the material flow better. After that, the FSP tool moved further from the right to the left side with definite PS. When the FSP tool reached at the endpoint, i.e. on the left side, then also dwell time of 15 seconds was provided to the FSP tool, so that retraction of the tool from the material became easy.

Processing of the plates was completed as per the process parameters shown in Table 3.7. FSP was successful, and sound processed plates were obtained, as shown in Figure 3.29. Three replicates were produced for each set of process parameters.

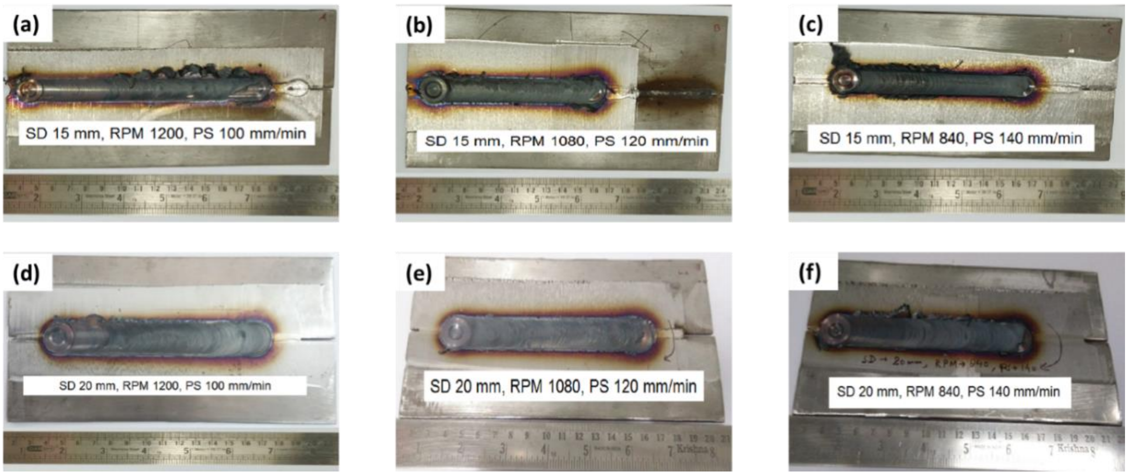

Figure 3.29 FSP of gas metal arc welded plate S7 at different processing parameters.

3.2.9 Characterisation of the processed plates

It was expected that the plates produced after FSP would be free of defects and with improved properties. Characterisation of the processed plates was carried out to examine the soundness of the plates after the processing operation and to evaluate the properties of the material after FSP. X-ray radiography was performed as the non-destructive test, and several tests such as metallographic study, hardness testing, tensile testing, Charpy impact testing and residual stress testing were carried out on the processed plates.

3.2.9.1 X-ray radiography

Although no visual defects were found on the processed plates, various types of defects, such as tunnel defect, the inclusion of tool wear debris, etc., may present within the processed plate. It is essential to test the FSPed plates for any subsurface defects. X-ray radiography is well known non-destructive testing technique to detect subsurface defects. All friction stir processed plates were subjected to 100% X-ray radiography.

3.2.9.2 Specimen extraction location from welded plates

Figure 3.30 shows the schematic diagram of the locations of different specimens extracted from the processed plates.

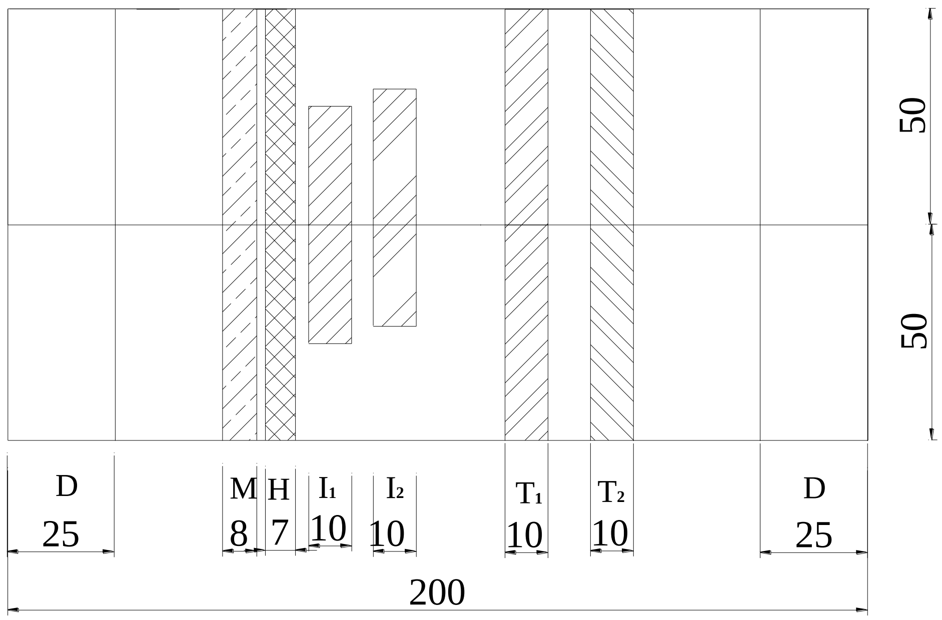

(All dimensions are in mm).

Figure 3.30 Schematic diagram of extraction of different specimens for characterisations from the processed plates.

To characterise the processed plates, different specimens such as metallographic samples for microstructural study (denoted by M) and hardness measurement (denoted by H), transverse tensile testing (denoted by T_1), reduced section tensile testing (denoted by T_2), and Charpy impact testing specimens I_1 and I_2 were extracted from the processed plates. Some part of the material was discarded from both ends of the processed plates, denoted by ‘D’.

3.2.9.3 Metallographic study

To carry out the metallographic study, the samples were first taken out, polished, and then etching of the samples were carried out to reveal the microstructure. The method of sample preparation and etching was the same as described earlier for the case of the welded plate. After etching the metallographic samples, the microstructures of different locations such as PR, TMAZ, HAZ and WMZ were captured with the help of an optical microscope. Micrography was carried out on the transverse section of the plates. Since the grains of the PRs had become finer due to FSP operation, to find the grain size of different regions, the microstructures of different locations have been captured using a scanning electron microscope (SEM) at 10,000 magnification. The procedure of finding the grain size has been already described in section 3.1.9.

3.2.9.4 Hardness testing

A hardness test was carried out on the transverse section of the plate as per ASTM E384 [182]. Microhardness was carried out, and indentations were made in and around the friction stir PR. The procedure for sample preparation and hardness testing was the same as when finding the microhardness of the welded plate, as described in section 3.1.9.

3.2.9.5 Tensile testing

Two types of tensile tests were performed; transverse tensile test and reduced section tensile test. To know the weakest region in the plate, transverse tensile specimens were prepared and tested and to know the strength of the PR, reduced section tensile specimen (with the reduced section in PR) were tested. The procedure and machine used for tensile testing were the same as used for the case of the welded plate (in section 3.1.9).

The broken transverse tensile sample and reduced section tensile sample after performing the tensile testing operation is shown in Figure 3.31 and Figure 3.32, respectively.

Figure 3.31 Fractured transverse tensile sample after performing tensile testing.

Figure 3.32 Fractured reduced section tensile sample after performing tensile testing.

3.2.9.6 Charpy impact testing

Two types of Charpy samples were prepared for this testing. In the first type of Charpy sample (I_1), the notch was present in the middle position of the stir zone and in the second type of Charpy sample (I_2) also, the notch was present in the PR but not in the middle position of the stir zone, instead of that the location of the notch is corresponding to the HAZ of the welded plate. From I_1, the toughness of the stir zone can be found, whereas I_2 can find the toughness improvement in the HAZ of the welded plate after carrying out the FSP operation. The procedure of sample preparation and machines used for this testing were the same as used for the welded plate.

3.2.9.7 Residual stress measurement of the processed plates

The measurement of the longitudinal residual stress at different locations of the PR along with the BMZ were carried out on the upper surface of the processed plate sample A.

The locations of measurement are shown schematically in Figure 3.33.

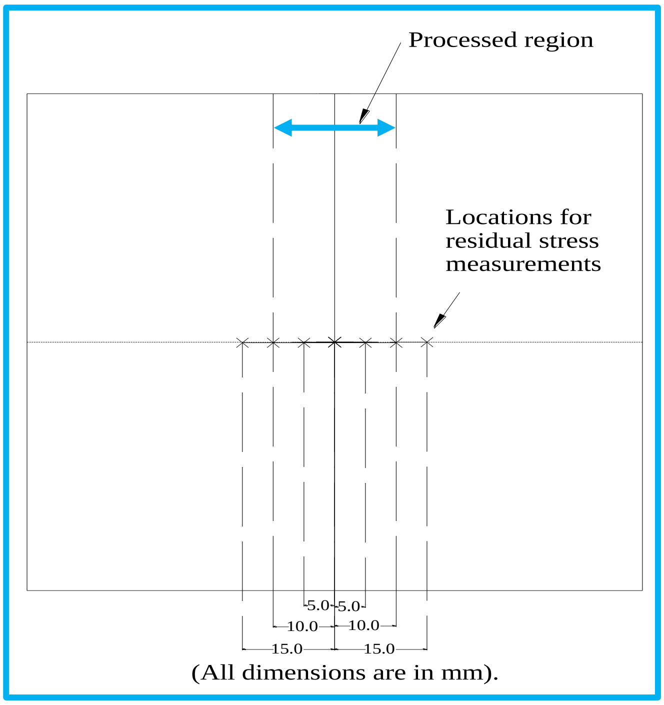

Figure 3.33 Schematic diagram showing residual stress measurement points in the processed plates.

3.2.9.8 Magnetic Barkhausen noise analysis

The magnetic Barkhausen noise (MBN) and magnetic hysteresis loop (MHL) response of the stir zone had been found by using an MBN analyser. The procedure and the machines used for this analysis was the same as used in the case of the welded plate.